

# Detection of naphthalene in sea-water by a label-free plasmonic optical fiber biosensor

Nunzio Cennamo<sup>1</sup>, Luigi Zeni<sup>1\*</sup>, Ezio Ricca<sup>2</sup>, Rachele Isticato<sup>2</sup> Vincenzo Manuel Marzullo<sup>3</sup>,  
Alessandro Capo<sup>4</sup>, Maria Staiano<sup>4</sup>, Sabato D'Auria<sup>4\*</sup>, and Antonio Varriale<sup>4</sup>

<sup>1</sup>Department of Engineering, University of Campania "Luigi Vanvitelli", 81031 Aversa, Italy

<sup>2</sup>Department of Biology, University of Naples Federico II, Complesso Universitario Monte Sant'Angelo, via Cinthia 4, 80126, Naples, Italy.

<sup>3</sup>Institute of Protein Biochemistry, IBP-CNR, Via Castellino 111, 80131 Napoli, Italy

<sup>4</sup>Institute of Food Science, ISA-CNR, Via Roma 64, 83100 Avellino, Italy

Corresponding Authors:

Dr. Sabato D'Auria

ISA-CNR

Via Roma, 52,

83100 Avellino

Tel. +39-0825299101

Fax: +39-0825 78158

Email: sabato.dauria@cnr.it

AND

Prof. Luigi Zeni

Department of Industrial and Information Engineering,

University of Campania "Luigi Vanvitelli", 81031 Aversa, Italy

Tel. +39-081-5010-269

Fax: +39- 081-5010-204

Email: luigi.zeni@unicampania.it

## Abstract

In this study we developed an optical fiber biosensor able to detect the presence of naphthalene in sea-water. With this aim, we designed and produced an antibody specific for the naphthalene molecule. The capability of the antibody to bind to naphthalene was characterized by ELISA tests. A surface plasmon resonance (SPR) sensor platform was realized by sputtering a gold layer on a modified plastic optical fiber (POF). The gold surface was derivatized and functionalized with the produced antibody by using the EDC/NHS amino-coupling immobilization protocol. The obtained results indicated that the POF-biosensor is able to sense the presence of naphthalene in a sea-water solution. The limit of detection (LOD) value was calculated to be 0.76 ng/mL, a value lower than the maximum residue limit value of naphthalene (0.13  $\mu\text{g/mL}$ ) referred as the water environmental quality standards (EQS). In addition, to the high sensitivity of the assay, it is remarkable to point out the possibility to monitor the presence of naphthalene in a real sea water solution by exploiting a simple experimental setup with a remote sensing capability offered by the POF-biosensor.

## Introduction

Naphthalene (NAPHTA) is a simple polycyclic aromatic hydrocarbon (PAH). Its structure is made by a fused pair of benzene rings, whose formula is  $C_{10}H_8$ . The U.S. Environmental Protection Agency (EPA) has rated naphthalene as a semi-volatile organic compound (SVOC) [1]. The International Agency for Research on Cancer (IARC), instead, focusing on the association to rare nasal tumours due to the exposition to naphthalene, has classified naphthalene as possibly carcinogenic to humans [2]. Releases of naphthalene are controlled through the Prevention and Control (PPC) Regulations, the Food and Environmental Protection Act (FEPA 1985), the Control of Pesticides Regulations (COPR 1986) and the UK Surface Waters (dangerous substances) Regulations (SI 1997/2560). At an international level, naphthalene is listed as a candidate substance for priority action under the Helsinki convention for the protection of the marine environment of the north-east Atlantic (OSPAR Conventions), in order to protect the marine environments of the Baltic Sea and north-east Atlantic Ocean. Eventually, the World Health Organization (WHO) is considering the development of an indoor air guideline for naphthalene pollution [3].

Naphthalene is naturally found in fossil fuels and the largest exposures to this compound occur near sources emitting naphthalene. The main anthropogenic sources of naphthalene are represented by chemical industries, burning of biomass, insect repellents and gasoline [4]. In urban areas, the main source of dangers for human health is the exposition to vehicle emissions containing high levels of naphthalene [5,6]. It is also reported that exposure for long time can affect the peripheral nervous system, kidneys and the liver. [7].

In order to detect the presence of NAPHTA in different real matrices, an analytical method is required. At present, capillary gas chromatography [8], gas chromatography-mass spectrometry [7, 9, 10] and high-performance liquid chromatography [11] are the main methods used for the determination of naphthalene. Gas chromatography coupled with infrared spectroscopy [12], gas chromatography with fluorescence detection [13], nuclear magnetic resonance spectrometry [14] and laser mass spectrometry [15] techniques have been developed. A crucial step for the naphthalene determination is represented by the need to perform a pre-concentration phase (both if analyses are performed in air or water samples) before its determination. This represents a bottleneck for the NAPHTA determination.

1 In this context, a biosensor may represent an interesting analytical tool to detect NAPHTA without  
2 pre-concentration or derivatization steps.

3 In order to achieve this purpose, we exploited an SPR sensor platform based on plastic optical fibers  
4 (POFs) [16]. We utilized as specific molecular recognition element (MRE) for NAPHTA a novel  
5 antibody able to detect NAPHTA in aqueous medium without any pre-concentration step.  
6

7 POF sensor systems are particularly advantageous due to their easily handling and installation  
8 procedures, large diameter of the fiber (a millimetre or more), low-cost and simplicity in  
9 manufacturing [16-25]. As reported in literature, SPR sensor based on a D-shaped POF [16] is  
10 particularly interesting for bio-sensing applications because it works with a planar gold surface and  
11 an external medium refractive index ranging from 1.33 to 1.42 values. These values are typical of  
12 biosensors used for specific detection of analytes in aqueous media by self-assembling monolayers  
13 [17, 21-25].  
14

15 In this work, we developed and characterized an SPR-POF biosensor to detect traces of NAPHTA  
16 in seawater samples. As previously developed for PFOA and other analytes [17,21-25] the gold  
17 surface of the SPR-POF sensor was chemically modified through the formation of specific reactive  
18 groups and functionalized with antibodies able to specifically recognize the NAPHTA. To obtain  
19 the anti- NAPHTA antibodies, a retro-synthetic chemical strategy was applied to modify the  
20 NAPHTA structure in a derivative structure. This modified NAPHTA structure was coupled to a  
21 protein carrier and used for immunization.  
22

23 The developed sensing assay allowed to perform measurements directly in real matrices of sea  
24 water. The results showed that the NAPHTA biosensor is able to sense the presence of 0.76 ppb  
25 NAPHTA, an amount lower than the limit value (0.13  $\mu\text{g/mL}$ ) fixed by European Union  
26 regulations.  
27  
28  
29  
30  
31  
32  
33  
34  
35  
36  
37  
38  
39  
40  
41  
42  
43  
44  
45  
46  
47  
48  
49  
50  
51  
52  
53  
54  
55  
56  
57  
58  
59  
60  
61  
62  
63  
64  
65

## Materials and Methods

### 2.1 Materials

N-hydroxysuccinimide (NHS), N-(3-dimethylaminopropyl)-N'-ethylcarbodiimide hydrochloride (EDC), Keyhole limpet hemocyanin (KLH) and  $\alpha$ -lipoic acid were purchased from Sigma-Aldrich (Sigma-Aldrich S.r.l. Milan, Italy). All the other chemicals were commercial samples of the purest quality.

### 2.2. Naphthalene derivative synthesis

Tetraethylene glycol p-toluenesulfonate (100 mg, 0,287 mmol) was added to a round-bottomed flask containing an ice-cold solution of 5 equivalents of N-Methyl-1-naphthalenemethylamine, in 500  $\mu$ L of anhydrous pyridine. The reaction was left to react for 30 minutes under magnetic stirring, then a gentle reflux was applied by heating the mixture with an oil bath. The colour of the reaction mix turned from transparent to pale yellow after the first 30 min, then into amber during the 2 h of reflux. Thin-layer chromatography (TLC) confirmed the formation of the product. The mixture was co-evaporated with anhydrous toluene to eliminate the pyridine, then it was purified by standard acid/base liquid separation to obtain a viscous amber oil, which was further purified by preparative silica TLC (8:2 DCM:MeOH + 0.1% NH<sub>3</sub> solution). The incorporation of the tetra-ethylene glycol linker was confirmed by nuclear magnetic resonance spectroscopy (NMR) experiment. Finally, the product was further transformed to be amino-reactive by incorporation of a reactive NHS moiety. The alcohol previously obtained was left to react overnight at 4°C under vigorous stirring with 1.2 equivalent of NaH, then iodoacetic acid (5 eq.) was added to the reaction mix. The crude product is then dried at rota-vapor and the mix was esterificated in DMF with 10 eq. of TEMED and 5 eq. of NHS. The obtained compound was characterized by <sup>1</sup>H-NMR and the characteristic resonances of the atomic group present in the structure were identified.

### 2.3 Keyhole Limpet Hemocyanin (KLH- NAPHTA) conjugates production

Keyhole limpet hemocyanin (KLH) is a large, multi-subunits, oxygen-carrying metallo-protein extensively used as a carrier protein in the production of antibodies. The KLH was purchased from the Thermo-Fisher and was used in conjugation reaction with the amino reactive naphthalene

1 produced. For the conjugation, the following procedure was used: Naphthalene derivative  
2 containing the reactive group for a fast self-coupling with proteins was dissolved in 10 mM  
3 phosphate buffer at pH 7.4 and incubated with the KLH protein, the molar ratio was 1:100. The  
4 reaction mixture was incubated at room temperature under continuous stirring for 2 hours and then  
5 dialyzed against 0.5 L of 10 mM phosphate buffer at pH 7.4 for 4 days with daily buffer changes.  
6 After the extensive dialysis the conjugate KLH-NAPHTA produced was used as antigen in the  
7 immunization procedure.  
8  
9  
10  
11  
12  
13

#### 14 *2.4 Immunization procedure and purification of IgG anti-Naphthalene*

15 Two rabbits were immunized following a standard protocol of immunization reported in Pennacchio  
16 et al. [26]. For this purpose, intradermal inoculation of KLH- NAPHTA conjugate (1 mg per each  
17 rabbit) was executed. At the end of the immunization process, the rabbits were sacrificed and their  
18 blood collected and centrifuged to separate blood cells from serum. The obtained sera were used for  
19 IgG anti-Naphthalene purification. Soon afterwards, the serum sample was diluted in ratio 1:1 with  
20 binding buffer (Tris-HCl 50 mM pH 7.4) and applied to Protein A resin (Sigma-Aldrich). After an  
21 overnight binding step, the flow-through was eluted and the wash step with 50 mM Tris-HCl pH 7.4  
22 was performed in order to remove the un-binding proteins from the column. After these steps, the  
23 IgG fractions were eluted from column with 0.1 M of Glycine-HCl pH 3.0 and immediately  
24 buffered using a solution of Tris-HCl 1.0 M pH 9.0. In order to estimate the homogeneity and the  
25 molar concentration of the purified total IgG, a gel electrophoresis in denatured condition (SDS-  
26 PAGE) and adsorption spectra were respectively made (data not shown).  
27  
28  
29  
30  
31  
32  
33  
34  
35  
36  
37  
38  
39

#### 40 *2.5 Affinity column preparation of NAPHTA -EAH Sepharose 4B and mono-specific antibody anti-* 41 *Naphtha purification*

42 The affinity column was obtained by conjugating the naphthalene derivative to EAH Sepharose 4B  
43 using the manufacturing instruction. In brief, a 12 mL sample of the resin was washed with H<sub>2</sub>O at  
44 pH 4.5 (160 mL), with 0.5M NaCl (100 mL), and again with H<sub>2</sub>O at pH 4.5 (100 mL). The  
45 Sepharose resin was finally packed into a polystyrene column (50 mL, BIORAD) suspended in 2.0  
46 mL of H<sub>2</sub>O at pH 4.5 and the resulting suspensions were gently shaken. The Naphthalene  
47 derivative, containing in its structure a reactive group for a fast self-coupling with proteins, was  
48 dissolved in 10 mM phosphate buffer at pH 7.4 and incubated with the slurry resin at a molar ratio  
49 of 1:10 for 2 h at room temperature. The slurry resin solution was extensively washed with H<sub>2</sub>O at  
50 pH 4.5, 0.5 M NaCl, then it was treated with 15 mL of 0.1 M AcOH at pH 4.0, 0.5 M NaCl  
51 (blocking buffer) and later with 0.1MTris-HCl at pH 7.0, 0.5 M NaCl (wash buffer). After this step,  
52  
53  
54  
55  
56  
57  
58  
59  
60  
61  
62  
63  
64  
65

1 the resin was washed with the blocking buffer and incubated for 30 min at room temperature.  
2 Finally, the resin was equilibrated with 10 mL of 50 mM Tris-HCl at pH 7.4. The total IgGs  
3 obtained from the Protein A purification step were incubated with the EAH-Naphtha resin  
4 produced. After the incubation step, the column was extensively washed with 50 mM Tris-HCl  
5 pH7.4 in order to remove un-specific binding with the EAH-NAPHTA resin of the IgGs. The  
6 mono-specific IgGs were eluted by strong pH changing (Glycine 50 mM pH 3.0) and the purity and  
7 binding capability of the obtained mono-specific antibodies were evaluated through the SDS-  
8 PAGE. Finally, the concentration of the antibodies at the end of dialyses processes was  
9 spectrophotometrically determined by absorbance measurements at  $\lambda = 278$  nm.  
10  
11  
12  
13  
14  
15  
16

### 17 *2.6 Glutamine-Binding protein- NAPHTA conjugate and ELISA test*

18 The antibodies titer was determined by using indirect ELISA assay, as reported by Pennacchio [26].  
19 In order to avoid interference from the carrier protein in the polyclonal antibody detection process,  
20 NAPHTA derivative (through the same procedure used for KLH- NAPHTA) was conjugated to the  
21 Glutamine binding protein isolated from E. coli [27]. The GlnBP- NAPHTA conjugate (2 mg/ml),  
22 prepared according to Pennacchio [26], diluted 1/200, was dissolved in coating buffer at pH 9.5 (25  
23 mM carbonate/bicarbonate) and was deposited on coat 96-well micro-plates surface in a range of  
24 concentrations from 1.2 ng/mL to 1.7 ng/mL, GlnBP with same concentration was dissolved in  
25 coating buffer and used as negative control. The plate was incubated overnight at 4°C. After this  
26 incubation, it was washed three-times with PBS buffer (0.1 M) containing 0.05% Tween (PBS-T),  
27 pH 7.4 and blocked for 1 hour at room temperature with a solution of 1% milk in PBS-T buffer. The  
28 wells were washed several times with PBS-T after each step, incubated with mono-specific anti-  
29 PFOA antibodies at 37°C for 1 hour and subsequently with horseradish peroxidase-conjugated anti-  
30 rabbit IgG antibodies (diluted 1:12000). This solution was incubated for 1 hour at 37°C. The  
31 enzyme substrate TMB was added, and the colour reaction was quenched after 5 minutes by the  
32 addition of 2.5 M HCl. The absorbance value at 450 nm was measured, plotting the reciprocal of the  
33 antibody dilution against absorbance.  
34  
35  
36  
37  
38  
39  
40  
41  
42  
43  
44  
45  
46  
47  
48  
49

### 50 *2.7 Plasmonic Platform in optical fiber with the experimental setup*

51 The optical platform was realized in a D-shaped plastic optical fiber (POF) sensing region, of 10  
52 mm in length, by a multilayer deposited on the flat exposed POF core (D-shaped sensing region).  
53

54 **The used POF showed a diameter of 1.0 mm, a core of poly-methyl methacrylate (PMMA) with 980**  
55  **$\mu\text{m}$  in size and a cladding of fluorinated polymer (20  $\mu\text{m}$  of size).**  
56  
57  
58

59 The procedure to obtain this plasmonic platform was based only on three steps: first, removing the  
60  
61  
62  
63  
64  
65

1  
2  
3  
4  
5  
6  
7  
8  
9  
10  
11  
12  
13  
14  
15  
16  
17  
18  
19  
20  
21  
22  
23  
24  
25  
26  
27  
28  
29  
30  
31  
32  
33  
34  
35  
36  
37  
38  
39  
40  
41  
42  
43  
44  
45  
46  
47  
48  
49  
50  
51  
52  
53  
54  
55  
56  
57  
58  
59  
60  
61  
62  
63  
64  
65

cladding of POF (along half circumference) by polishing process; second, spin coating (6,000 rpm for 60 seconds) an optical buffer layer on the POF core; finally, sputtering a thin gold film by a Bal-Tec SCD 500 machine. The sputtering process was repeated three times by applying a current of 60 mA for 35 seconds (20 nm of gold for step).

The proposed buffer layer, used to improve the performances and the adherence of the gold film, was a photoresist Microposit S1813, with a refractive index greater than the one of the POF core [16]. To deposit the photoresist buffer layer, we used a spin coater machine in order to obtain a uniform layer. Furthermore, the shape of the resonance curve and the absence of multiple resonance peaks, obtained with the bare gold surface in water, were indirect indications of the uniformity of the photoresist buffer layer. In particular, the multilayer deposited on the D-shaped POF region presented a thickness of the buffer layer of about 1.5  $\mu\text{m}$  and a gold film of 60 nm.

The optical sensor system was completed with a very small size, simple and low-cost equipment, composed by a halogen lamp and a spectrometer connected to a PC. The white light source (halogen lamp, HL-2000-LL, manufactured by Ocean Optics, Dunedin, FL, USA) had an emission range from 360 nm to 1700 nm, whereas the spectrometer (FLAME-S-VIS-NIR-ES, manufactured by Ocean Optics, Dunedin, FL, USA) had a detection range from 350 nm to 1023 nm. We connected the SPR-POF sensor to the equipment, light source and spectrometer by two removable SMA connectors. The SPR curves along with data values were displayed on-line on the computer screen and saved with the help of a software provided by Ocean Optics, setting the integration time at 1,000  $\mu\text{s}$  and the averaging of the scans at 100. The SPR transmission spectra were normalized to the reference spectrum (air as the surrounding medium) by Matlab software [16].

### 2.8 Immobilization process on the chip surface

Following the immobilization procedure reported in Cennamo *et al* [17], the POF surface was sequentially cleaned with: (1) milli-Q water (3 times for 5 minutes) and (2) 10 % of ethanol solution in milli-Q water (3 times for 5 min). Then the surface was pre-treated before the covalently immobilization of mono-specific antibody against NAPHTA. This procedure consists of three different steps: (1) thiol film production, (2) derivatization of the surface by EDC/NHS (3) antibody anti-Naphthalene (anti-NAPHTA) immobilization. Soon afterwards the gold chip was immersed in freshly prepared solution of  $\alpha$ -lipoic acid dissolved in a solution of pure ethanol 10 % in water at the final concentration of 40 mM and incubated at 25°C for 18 h and after this incubation period, the gold-coated surface was washed with milli-Q water (three times). Sequentially, a mixture of EDC/NHS at the final concentrations of 200 mM and 50 mM, were incubated on the chip surface for 20 minutes at RT, then for 2 h at room temperature with an msAb anti-NAPHTA 2 mg/ml (100

1  
2  
3  
4  
5  
6  
7  
8  
9  
10  
11  
12  
13  
14  
15  
16  
17  
18  
19  
20  
21  
22  
23  
24  
25  
26  
27  
28  
29  
30  
31  
32  
33  
34  
35  
36  
37  
38  
39  
40  
41  
42  
43  
44  
45  
46  
47  
48  
49  
50  
51  
52  
53  
54  
55  
56  
57  
58  
59  
60  
61  
62  
63  
64  
65

μl) solution in sodium phosphate buffer 20 mM, pH 7.5. Finally, the chips were washed with potassium phosphate buffer sodium phosphate buffer 20 mM, pH 7.5 and dried with nitrogen gas.

The immobilization process can be observed by the resonance wavelength, when a buffer solution (blank) is present as bulk. In fact, when a bio-layer is added to the gold film, the measured refractive index increases and the resonance wavelength increases, though there is an equal medium as bulk (buffer solution). The shift value due to the antibodies immobilization (post functionalization) was about 15 nm and about 20 nm after the final passivation step. This method has already been reported in our previous work [17].

### 2.9 Naphthalene sample preparation

2 mg/mL of naphthalene crystalline powder was solved into 2 mL of ethanol. 100 μL of this solution was diluted in 10 mL of deionized water. Then the water solution obtained (10 μg/mL naphthalene, 1% ethanol), was sequentially diluted to prepare the samples in a range of concentration from 2.5 to 0.0005 μg/mL. **The simulated sea-water matrix samples (in the same range of naphthalene concentration) were obtained by diluting 10 μg/mL naphthalene in 1% ethanol solution with 0,460 M NaCl buffer.**

### 2.10 Binding experiments

Experimental results were collected using a simple measuring protocol: about 50 μL of NAPHTA solutions at different concentrations were dropped over the sensing region; after an incubation step (ten minutes at room temperature for bio-interaction between analytes and receptor), a washing step with PBS (buffer) was carried out before the recording of the spectrum (when buffer is present as bulk). This protocol was used to measure the shift of the resonance determined by the specific binding (analyte/receptor interaction) on the sensing area, and not determined by the bulk refractive index changes or by non-specific binding between the gold surface and the analyte. The binding between the receptor on the SPR-POF platform and NAPHTA in real matrices was evaluated in the range from 0.0 to 2500 ppb (2.5 μg/mL).

### 3. Results and Discussion

#### 3.1 Antibody anti- NAPHTA design and production

During the last decade, a general strategy to activate and bind small analytes to an antigenic carrier was developed to produce high specific MREs such as antibody biomolecules [25-32]. This strategy, shown in **Figure 1**, starts from the functionalization of analytes to obtain a more reactive carboxylic/amino derivative for the conjugation with a carrier protein. This strategy gives an immunogenic molecule that produces a significantly higher immunological response. The immunogenic molecule obtained is then used for the production of antibodies.

In this context, a soluble NAPHTA derivative compound was been generated with the aim to obtain antibody molecules able to bind NAPHTA with high affinity. In particular, a retro-synthetic strategy was been planned and three main features were considered: 1) the derivative molecule should have an intact naphthalene scaffold; 2) the derivative molecule should be a not-immunogenic linker for a high water solubility and maintain a correct orientation; 3) the linker should have a reactive moiety for a fast self-coupling with proteins.

Following this strategy in **Figure 2** are reported the  $^1\text{H}$  NMR spectra (**Figure 2A**) and structure of the derivative compound (**Figure 2B**), obtained with the retrosynthetic approach described in the material and method section. The NAPHTA derivative containing a reactive group for a fast self-coupling with proteins was conjugated to the high immunogenic protein keyhole limpet hemocyanin (KLH). The obtained KLH-NAPHTA (**Figure 2C**) conjugate was used to produce a high-affinity antibody, using a standard protocol of immunization. At the end of this process, anti-NAPHTA antibodies (msAb-NAPHTA) were purified from serum through two different chromatography steps (Protein A Sepharose and NAPHTA-EAH Sepharose). Their binding capability to NAPHTA was evaluated. To estimate the titer of the msAb against NAPHTA, an indirect ELISA test was performed. In order to avoid interference from the carrier protein, in the ELISA test, NAPHTA derivative was conjugated to different carrier molecules. For this purpose the GlnBP isolated from *E. coli* was used. Microplate wells were coated with different concentrations of antigens GlnBP-NAPHTA and reacted with serially diluted msAb-NAPHTA. **Figure 3** shows the ELISA results, where the absorbance values at 450 nm are reported, for different concentrations of coated GlnBP-NAPHTA. No signal was registered from non-coated wells, while a positive signal was observed when the msAb dilution of 1 in 12,000 was applied. In order to test the antibody selectivity, the ELISA was also performed using as potential antigens different molecules that are known to be co-pollutants in the seawater, (e.g. PFOA and PFOS) and no cross-reactivity was found.

1  
2  
3  
4  
5  
6  
7  
8  
9  
10  
11  
12  
13  
14  
15  
16  
17  
18  
19  
20  
21  
22  
23  
24  
25  
26  
27  
28  
29  
30  
31  
32  
33  
34  
35  
36  
37  
38  
39  
40  
41  
42  
43  
44  
45  
46  
47  
48  
49  
50  
51  
52  
53  
54  
55  
56  
57  
58  
59  
60  
61  
62  
63  
64  
65

In **Figure 4** the SPR-POF sensor platform with the flow-chart used for the realization is shown. The obtained optical sensor system is small in size, simple and low-cost, being equipped with a halogen lamp and a spectrometer connected to a PC, as already reported in the Section 2.7.

In **Figure 5** the functionalization of the gold surface of the SPR-POF platform is reported. Aiming at obtaining a smart surface to detect the NAPHTA compound, as reported in our previous works [17, 25], the gold surface was sequentially treated with a solution of  $\alpha$ -lipoic acid (a), EDC/NHS (b) and finally with mono-specific antibodies against the NAPHTA (c). At the end of these steps, a passivation procedure of the surface was performed by incubation of GlnBP for 2 h at room temperature (**Figure 5A**). The immobilization of the antibodies on the sensor surface is confirmed by the SPR results: SPR transmission spectra, reported in **Figure 5B**, show a shift (an increase of the resonance wavelength) in presence of the same bulk refractive index, before and after the functionalization procedure. As already reported in Section 2.8, this shift, due to an increase of the refractive index in contact with the gold surface, indicates that the anti- NAPHTA antibodies were immobilized on the gold surface. **Figure 5B** shows a resonance shift value, after the functionalization step, of about 15 nm while the shift amounts to 20 nm after the final passivation step.

### 3.2 NAPHTA detection

In an SPR-POF platform when the refractive index at the gold-dielectric interface increases, the resonance wavelength shifts to the right (increase). When a bio-receptor layer is present on the gold film, the selective recognition and the consequent capture of the target analytes present in a liquid sample, lead to a local increase of the refractive index of the dielectric layer in contact with the metal, therefore the resonance wavelength increases. **Figure 6A** shows the transmission spectra of the SPR-POF with the bio-receptor, normalized to the reference spectrum (with air as the surrounding medium), and obtained at increasing concentrations of NAPHTA in a real sea-water solution. The resonance wavelength is shifted to higher values by increasing the concentration of the analyte (Fig. 6A). **Figure 6B** reports the variation of the resonance wavelength with respect to the blank,  $\Delta\lambda_c$  (nm), versus the analyte amount (ppm), in a semi-log scale, and the fitting by Hill equation reported below [33]:

$$\Delta\lambda_c = \Delta\lambda = \lambda_c - \lambda_0 = \Delta\lambda_{max} \cdot \frac{c^n}{K^n + c^n} \quad (1)$$

where  $\Delta\lambda_{max}$  is the maximum resonance wavelength variation at increasing concentration of

naphthalene (the saturation value minus the blank value). The symbol  $c$  indicates the concentration of the analyte and  $\lambda_c$  indicates the resonance wavelength at  $c$  concentrations. The resonance at 0.0ppb concentration (blank) is indicated as  $\lambda_0$ . The two parameters  $K$  and  $n$  are considered as descriptors of the standardization curve (Eq. 1), but they can also have a physical meaning [33]. Standardization curves, as the curves described by eq. 1, are commonly used when dealing with chemical sensors and biosensors. Their physical meaning, in particular the non-linear trend, is related to the finite number of the specific sites available for adsorption, which leads to a saturation at high analyte concentrations. In this case, the adsorption takes place according to the Langmuir adsorption isotherm [33]. The value of  $n$  in the Langmuir sorption model should be equal to 1, and it is different in case of the presence of cooperative effects.

In **Figure 6B**, each experimental point (black square) is the average of 5 subsequent measurements and the error bars represent the respective standard deviations, whereas the fitting is performed applying by fitting the Hill equation (OriginPro 8.5, Origin Lab. Corp., Northampton, MA, USA). The obtained parameters are listed in **Table 1**.

The  $\Delta\lambda_0$  value should be not significantly different from 0.0, since it indicates the shift of the resonance wavelength with the concentration of analyte at 0.0 ppb concentration. The value of  $n$  cannot be considered as significantly different from 1.0 (see **Table 1**). From Eq. 1 it is possible to notice that, if  $n \approx 1$  and at low concentration, i.e. at  $c$  much lower than  $K$ , the dose-response curve is linear, with sensitivity  $\Delta\lambda_{\max}/K$ , defined as the "sensitivity at low concentration", as shown in Eq. 2:

$$\Delta\lambda_c = \frac{\Delta\lambda_{\max}}{K} \cdot c \quad (2)$$

Standardization curves, like the curves reported in **Figure 6B**, with the Hill parameters listed in **Table 1**, are commonly used for biosensors. When the number of receptor sites available for the combination with the substrate is limited, the physical meaning of the Hill's parameters can be related to the fact that the adsorption takes place by the combination of the substrate at specific sites (the adsorption takes place according to the Langmuir adsorption isotherm). The parameter  $K$  of the Hill equation (Eq. 1 and 2) corresponds to the reciprocal of the affinity constant of the specific sites of the Langmuir model [33]. The affinity constant ( $K_{\text{aff}}$ ), the sensitivity at low concentration and the lower detection limits (LOD) of naphthalene in a real sea-water solution are reported in **Table 2**. The LOD can be calculated by the ratio of three times the standard deviation of the blank.

In order to verify the non-specific binding between the sensing layer and the NAPHTA, the response of SPR-POF sensor without the bio-receptor was tested. **Figure 7** shows the SPR curves

1  
2  
3  
4  
5  
6  
7  
8  
9  
10  
11  
12  
13  
14  
15  
16  
17  
18  
19  
20  
21  
22  
23  
24  
25  
26  
27  
28  
29  
30  
31  
32  
33  
34  
35  
36  
37  
38  
39  
40  
41  
42  
43  
44  
45  
46  
47  
48  
49  
50  
51  
52  
53  
54  
55  
56  
57  
58  
59  
60  
61  
62  
63  
64  
65

obtained with different concentrations of NAPHTHA in real solution. In this case, we used a range of NAPHTHA concentration wider than the saturation value (around 10 ppb). The results obtained show that, as a consequence of the concentration increase, the shift of the resonance wavelength was not registered.

#### 4. Conclusion

Aiming at detecting naphthalene in seawater, we designed a novel SPR-POF sensor that combines a novel antibody layer with a plasmonic platform in plastic optical fibers. The procedure used for the bio-receptor design and production allows to obtain very high affinity antibodies against the NAPHTHA and this characteristic was used to develop the SPR-POF biosensor. The binding tests were realized on laboratory and simulated real matrix samples. The selective recognition of NAPHTHA, in a liquid sample by antibody layer, displayed an increase of the resonance wavelength.

The obtained results showed that the assay is selective and able to sense the presence of a very low amount of NAPHTHA, exhibiting a LOD of 0.76 ng/mL (0.76 ppb), a value that is lower than the one fixed by the European Union regulations. In the future, after these preliminary laboratory results, the remote sensing capabilities offered by optical fibers could be exploited for on-site and real-time monitoring of the naphthalene concentration in sea-water.

#### Acknowledgments

This work was funded by the EUFP7 program under grant agreement N° 614088- Mariabox project.

## Reference

- [1] USEPA, compendium of methods for determination of toxic organic compounds in ambient air, Center for Environmental Research Information; Office of Research and Development, U.S. Environmental Protection Agency; Cincinnati, OH 45268 Second Edition (January, 1999).
- [2] WHO, IARC Monographs on the evaluation of carcinogenic risks to humans - some traditional herbal medicines, some mycotoxins, naphthalene and styrene, ed.82, IARC Press, Lyon, France (2002).
- [3] WHO, Development of WHO Guidelines for indoor air quality, WHO Regional Office for Europe, Copenhagen, Denmark (2006).
- [4] C.R. Jia, S. Batterman, A critical review of naphthalene sources and exposures relevant to indoor and outdoor air, *Int. J. Environ. Res. Public Health* 7 (2010) 2903-2939.
- [5] J.J. Schauer, M.J. Kleeman, G.R. Cass, B.R. Simoneit, Measurement of emissions from air pollution sources. 5. C1-C32 organic compounds from gasoline-powered motor vehicles, *Environ Sci Technol* 36(6) (2002) 1169-80.
- [6] S.D. Shah, T.A. Ogunyoku, J.W. Miller, D.R. Cocker, 3rd, On-road emission rates of PAH and n-alkane compounds from heavy-duty diesel vehicles, *Environ Sci Technol* 39(14) (2005) 5276-84.
- [7] Helvécio C. Menezes, Breno P. Paulo, Nathália T. Costa, Z.L. Cardeal, New method to determination of naphthalene in ambient air using cold fiber-solid phase microextraction and gas chromatography-mass spectrometry *Microchemical Journal* 109 (2013) 93-97.
- [8] K. Hasegawa, H. Nozawa, I. Yamagishi, K. Watanabe, S. O., Simple analysis of naphthalene in human whole blood and urine by headspace capillary gas chromatography with large-volume injection, *Forensic Toxicology* 27(2) (2009) 98-102.
- [9] R. Lindahl, A.S. Claesson, M.A. Khan, J.O. Levin, Development of a method for the determination of naphthalene and phenanthrene in workplace air using diffusive sampling and thermal desorption GC-MS analysis, *Ann Occup Hyg* 55(6) (2011) 681-7.
- [10] M.A. Hossain, F. Yeasmin, S.M.M. Rahman, M.S. Rana, Gas chromatograph-mass spectrometry determination of carcinogenic naphthalene, anthracene, phenanthrene and fluorene in the Bangsai river water of Bangladesh, *Arabian Journal of Chemistry* 9(1) (2016) S109-S113.
- [11] J.M. Shamar, Separation and identification of naphthalene, acenaphthylene, pyrene, benz{a}anthracene and 1,3,2,4-dibenzanthracene, *Journal of Al-Nahrain University* 12 (4) (December, 2009) 14-24
- [12] Cheng-Yu Wang, Frank and Edwards, K. E., Separation of C2-naphthalenes by gas chromatography Fourier transform infrared spectroscopy (GC FT-IR): Two-Dimensional Separation Approach, *Anal. Chem.* 79 (2007) 106-112.
- [13] John M. Hayes, G.J. Small, rotationally cooled laser-induced fluorescence/gas chromatography, *Anal. Chem.* 54( 7) (1982) 1202-1204.
- [14] Nicola Zanca, Andrew T. Lambe, Paola Massoli, Marco Paglione, David R. Croasdale, Yatish Parmar, Emilio Tagliavini, Stefania Gilardoni, a.S. Decesari, Characterizing source fingerprints and ageing processes in laboratory-generated secondary organic aerosols using proton-nuclear magnetic resonance (1H-NMR) analysis and HPLC HULIS determination, *Atmos. Chem. Phys.* 17 (2017) 10405-10421.
- [15] Ulrich Boesl, Laser mass spectrometry for environmental and industrial chemical trace analysis, *Journal of mass spectrometry* 35(3) (2000) 289-304.
- [16] N. Cennamo, D. Massarotti, L. Conte, L. Zeni, Low cost sensors based on SPR in a plastic optical fiber for biosensor implementation, *Sensors (Basel)* 11(12) (2011) 11752-60.
- [17] N. Cennamo, L. Zeni, P. Tortora, M.E. Regonesi, A. Giusti, M. Staiano, S. D'Auria, A. Varriale, A high sensitivity biosensor to detect the presence of perfluorinated compounds in environment, *Talanta* 178 (2018) 955-961.

- 1 [18] L. Bilro, N. Alberto, J.L. Pinto, R. Nogueira, Optical sensors based on plastic fibers, *Sensors* 12 (2012) 12184-12207.
- 2 [19] Y. Jin, A. M. Granville, Polymer Fiber Optic Sensors - A Mini Review of their synthesis and  
3 applications, *J. Biosens. Bioelectron.* 7: 194 (2016) 1-11.
- 4 [20] V.V.R. Sai, T. Kundu, S. Mukherji, Novel U-bent fiber optic probe for localized surface  
5 plasmon resonance based biosensor, *Biosens Bioelectron* 24 (2009) 2804.
- 6 [21] N. Cennamo, A. Varriale, A. Pennacchio, M. Staiano, D. Massarotti, L. Zeni, S. D'Auria, An  
7 innovative plastic optical fiber based biosensor for new bio/applications. The case of celiac disease,  
8 *Sens. Act. B: Chem.* 176 (2013) 1008–1014.
- 9 [22] N. Cennamo, G. Alberti, M. Pesavento, G. D'Agostino, F. Quattrini, R. Biesuz, L. Zeni, A  
10 simple small size and low cost sensor based on surface plasmon resonance for selective detection of  
11 Fe(III), *Sensors* 14 (2014) 4657-4671.
- 12 [23] N. Cennamo, M. Pesavento, L. Lunelli, L. Vanzetti, C. Pederzoli, L. Zeni, L. Pasquardini, An  
13 easy way to realize SPR aptasensor: A multimode plastic optical fiber platform for cancer  
14 biomarkers detection, *Talanta* 140 (2015) 88–95.
- 15 [24] A. Aray, F. Chiavaioli, M. Arjmand, C. Trono, S. Tombelli, A. Giannetti, N. Cennamo, M.  
16 Soltanolkotabi, L. Zeni, F. Baldini, SPR-based plastic optical fibre biosensor for the detection of C-  
17 reactive protein in serum, *J Biophotonics* 9 (2016)1077–1084.
- 18 [25] N. Cennamo, S. Di Giovanni, A. Varriale, M. Staiano, F. Di Pietrantonio, A. Notargiacomo, L.  
19 Zeni, S. D'Auria, Easy to use plastic optical fiber-based biosensor for detection of butanal, *PLoS*  
20 *ONE* 10(3) (2015) e0116770.
- 21 [26] A. Pennacchio, A. Varriale, M.G. Esposito, A. Scala, V.M. Marzullo, M. Staiano, S. D'Auria,  
22 A rapid and sensitive assay for the detection of benzylpenicillin (PenG) in milk, *PLoS ONE* 10(7)  
23 (2015) e0132396.
- 24 [27] M. Staiano, V. Scognamiglio, M. Rossi, S. D'Auria, O.V. Stepanenko, I.M. Kuznetsova, K.K.  
25 Turoverov, Unfolding and refolding of the glutamine-binding protein from *Escherichia coli* and its  
26 complex with glutamine induced by guanidine hydrochloride, *Biochemistry* 44(15) (2005) 5625-33.
- 27 [28] M. De Champdoré, P. Bazzicalupo, L. De Napoli, D. Montesarchio, G. Di Fabio, I. Coccozza,  
28 A. Parracino, M. Rossi, S. D'Auria, A new competitive fluorescence assay for the detection of  
29 patulin toxin, *Anal Chem* 15(79(2) ) (2007) 751-757.
- 30 [29] A. Varriale, V.M. Marzullo, S. Di Giovanni, A. Scala, A. Capo, A. Majoli, A. Pennacchio, M.  
31 Staiano, S. D'Auria, On the possibility of ephedrine detection: time-resolved fluorescence resonance  
32 energy transfer (FRET)-based approach, *Anal Bioanal Chem* 408(23) (2016) 6329-36.
- 33 [30] S. Di Giovanni, A. Varriale, V.M. Marzullo, G. Ruggiero, M. Staiano, A. Secchi, L. Pierno,  
34 A.M. Fiorello, S. D'Auria, Determination of benzyl methyl ketone - a commonly used precursor in  
35 amphetamine manufacture, *Anal. Methods* 4 (2012) 3558-3564.
- 36 [31] A. Varriale, K. Bonnot, S. Peransi, A. Scala, S. D'Auria, Self-oriented monolayer  
37 immobilization of ovalbumin and *B. cereus* antibody molecules on a chemically modified surface of  
38 silicon nitride fosters the enhancement of capture of bio-agents, *Colloids Surf B Biointerfaces* 148  
39 (2016) 585-591.
- 40 [32] A. Pennacchio, A. Varriale, M.G. Esposito, M. Staiano, S. D'Auria, A near-infrared  
41 fluorescence assay method to detect patulin in food, *Anal Biochem* 481 (2015) 55-9.
- 42 [33] B.I. Burganov, A.V. Lobanov, I.A. Borisov, A.N. Reshetilov, Criterion for Hill equation  
43 validity for description of biosensor calibration curves, *Anal. Chim. Acta* 427 (2001) 11-19.
- 44  
45  
46  
47  
48  
49  
50  
51  
52  
53  
54  
55  
56  
57  
58  
59  
60  
61  
62  
63  
64  
65

1  
2  
3 **Figure legend**  
4

5 **Figure 1.** Flowchart of the strategy used for antibodies production, purification and quantification.  
6

7 **Figure 2.** (A) <sup>1</sup>H NMR spectrum of the naphthalene derivative. (B) Water soluble and self-  
8 conjugate naphthalene derivative. (C) 2. Scheme of conjugation reaction between the KLH and  
9 naphthalene derivative, the reaction was performed at RT, at pH 6.0 for 2 h.  
10  
11

12 **Figure 3.** Indirect ELISA test results obtained using msAb anti-NAPTHA. The assay was  
13 performed in the Tris-borate buffer in the presence of 0.005% Tween and 1% milk. Temperature  
14 was 25 °C.  
15

16 The dilution of anti-NAPTHA was 1:12,000.  
17

18 **Figure 4.** Plasmonic platform in POF with the experimental setup and the description of the needed  
19 steps to realize it.  
20  
21

22 **Figure 5.** Gold surface functionalization processes. Resonance spectra were acquired in buffer  
23 solution (PBS) obtained before and after the functionalization and passivation processes.  
24  
25

26 **Figure 6.** SPR spectra acquired to naphthalene detection. (A) SPR spectra obtained by SPR-POF  
27 *with* the bio-receptor at different concentrations of naphthalene in real seas water matrices (460 mM  
28 NaCl), in the range from 0.0 to 2500 ppb. (B) Plasmon resonance wavelength shift ( $\Delta\lambda_c$ ) versus  
29 concentration of naphthalene (ppb) in semi-logarithmic axes, and Hill equation fitting of the  
30 experimental data.  
31  
32

33  
34 **Figure 7.** SPR spectra obtained by SPR-POF *without the* bio-receptor at different concentrations of  
35 naphthalene in real sea-water matrices.  
36  
37  
38  
39  
40  
41  
42  
43  
44  
45  
46  
47  
48  
49  
50  
51  
52  
53  
54  
55  
56  
57  
58  
59  
60  
61  
62  
63  
64  
65

# Detection of naphthalene in sea-water by a label-free plasmonic optical fiber biosensor

Nunzio Cennamo<sup>1</sup>, Luigi Zeni<sup>1\*</sup>, Ezio Ricca<sup>2</sup>, Rachele Isticato<sup>2</sup> Vincenzo Manuel Marzullo<sup>3</sup>,  
Alessandro Capo<sup>4</sup>, Maria Staiano<sup>4</sup>, Sabato D'Auria<sup>4\*</sup>, and Antonio Varriale<sup>4</sup>

<sup>1</sup>Department of Engineering, University of Campania "Luigi Vanvitelli", 81031 Aversa, Italy

<sup>2</sup>Department of Biology, University of Naples Federico II, Complesso Universitario Monte Sant'Angelo, via Cinthia 4, 80126, Naples, Italy.

<sup>3</sup>Institute of Protein Biochemistry, IBP-CNR, Via Castellino 111, 80131 Napoli, Italy

<sup>4</sup>Institute of Food Science, ISA-CNR, Via Roma 64, 83100 Avellino, Italy

Corresponding Authors:

Dr. Sabato D'Auria

ISA-CNR

Via Roma, 52,

83100 Avellino

Tel. +39-0825299101

Fax: +39-0825 78158

Email: sabato.dauria@cnr.it

AND

Prof. Luigi Zeni

Department of Industrial and Information Engineering,

University of Campania "Luigi Vanvitelli", 81031 Aversa, Italy

Tel. +39-081-5010-269

Fax: +39- 081-5010-204

Email: luigi.zeni@unicampania.it

## Abstract

1  
2  
3 In this study we developed an optical fiber biosensor able to detect the presence of naphthalene in  
4 sea-water. With this aim, we designed and produced an antibody specific for the naphthalene  
5 molecule. The capability of the antibody to bind to naphthalene was characterized by ELISA tests.  
6  
7 A surface plasmon resonance (SPR) sensor platform was realized by sputtering a gold layer on a  
8 modified plastic optical fiber (POF). The gold surface was derivatized and functionalized with the  
9 produced antibody by using the EDC/NHS amino-coupling immobilization protocol. The obtained  
10 results indicated that the POF-biosensor is able to sense the presence of naphthalene in a sea-water  
11 solution. The limit of detection (LOD) value was calculated to be 0.76 ng/mL, a value lower than  
12 the maximum residue limit value of naphthalene (0.13  $\mu\text{g/mL}$ ) referred as the water environmental  
13 quality standards (EQS). In addition, to the high sensitivity of the assay, it is remarkable to point  
14 out the possibility to monitor the presence of naphthalene in a real sea water solution by exploiting  
15 a simple experimental setup with a remote sensing capability offered by the POF-biosensor.  
16  
17  
18  
19  
20  
21  
22  
23  
24  
25  
26  
27  
28  
29  
30  
31  
32  
33  
34  
35  
36  
37  
38  
39  
40  
41  
42  
43  
44  
45  
46  
47  
48  
49  
50  
51  
52  
53  
54  
55  
56  
57  
58  
59  
60  
61  
62  
63  
64  
65

## Introduction

Naphthalene (NAPHTA) is a simple polycyclic aromatic hydrocarbon (PAH). Its structure is made by a fused pair of benzene rings, whose formula is  $C_{10}H_8$ . The U.S. Environmental Protection Agency (EPA) has rated naphthalene as a semi-volatile organic compound (SVOC) [1]. The International Agency for Research on Cancer (IARC), instead, focusing on the association to rare nasal tumours due to the exposition to naphthalene, has classified naphthalene as possibly carcinogenic to humans [2]. Releases of naphthalene are controlled through the Prevention and Control (PPC) Regulations, the Food and Environmental Protection Act (FEPA 1985), the Control of Pesticides Regulations (COPR 1986) and the UK Surface Waters (dangerous substances) Regulations (SI 1997/2560). At an international level, naphthalene is listed as a candidate substance for priority action under the Helsinki convention for the protection of the marine environment of the north-east Atlantic (OSPAR Conventions), in order to protect the marine environments of the Baltic Sea and north-east Atlantic Ocean. Eventually, the World Health Organization (WHO) is considering the development of an indoor air guideline for naphthalene pollution [3].

Naphthalene is naturally found in fossil fuels and the largest exposures to this compound occur near sources emitting naphthalene. The main anthropogenic sources of naphthalene are represented by chemical industries, burning of biomass, insect repellents and gasoline [4]. In urban areas, the main source of dangers for human health is the exposition to vehicle emissions containing high levels of naphthalene [5,6]. It is also reported that exposure for long time can affect the peripheral nervous system, kidneys and the liver. [7].

In order to detect the presence of NAPHTA in different real matrices, an analytical method is required. At present, capillary gas chromatography [8], gas chromatography-mass spectrometry [7, 9, 10] and high-performance liquid chromatography [11] are the main methods used for the determination of naphthalene. Gas chromatography coupled with infrared spectroscopy [12], gas chromatography with fluorescence detection [13], nuclear magnetic resonance spectrometry [14] and laser mass spectrometry [15] techniques have been developed. A crucial step for the naphthalene determination is represented by the need to perform a pre-concentration phase (both if analyses are performed in air or water samples) before its determination. This represents a bottleneck for the NAPHTA determination.

1 In this context, a biosensor may represent an interesting analytical tool to detect NAPHTA without  
2 pre-concentration or derivatization steps.

3 In order to achieve this purpose, we exploited an SPR sensor platform based on plastic optical fibers  
4 (POFs) [16]. We utilized as specific molecular recognition element (MRE) for NAPHTA a novel  
5 antibody able to detect NAPHTA in aqueous medium without any pre-concentration step.  
6  
7

8 POF sensor systems are particularly advantageous due to their easily handling and installation  
9 procedures, large diameter of the fiber (a millimetre or more), low-cost and simplicity in  
10 manufacturing [16-25]. As reported in literature, SPR sensor based on a D-shaped POF [16] is  
11 particularly interesting for bio-sensing applications because it works with a planar gold surface and  
12 an external medium refractive index ranging from 1.33 to 1.42 values. These values are typical of  
13 biosensors used for specific detection of analytes in aqueous media by self-assembling monolayers  
14 [17, 21-25].  
15  
16

17 In this work, we developed and characterized an SPR-POF biosensor to detect traces of NAPHTA  
18 in seawater samples. As previously developed for PFOA and other analytes [17,21-25] the gold  
19 surface of the SPR-POF sensor was chemically modified through the formation of specific reactive  
20 groups and functionalized with antibodies able to specifically recognize the NAPHTA. To obtain  
21 the anti- NAPHTA antibodies, a retro-synthetic chemical strategy was applied to modify the  
22 NAPHTA structure in a derivative structure. This modified NAPHTA structure was coupled to a  
23 protein carrier and used for immunization.  
24  
25

26 The developed sensing assay allowed to perform measurements directly in real matrices of sea  
27 water. The results showed that the NAPHTA biosensor is able to sense the presence of 0.76 ppb  
28 NAPHTA, an amount lower than the limit value (0.13  $\mu\text{g/mL}$ ) fixed by European Union  
29 regulations.  
30  
31  
32  
33  
34  
35  
36  
37  
38  
39  
40  
41  
42  
43  
44  
45  
46  
47  
48  
49  
50  
51  
52  
53  
54  
55  
56  
57  
58  
59  
60  
61  
62  
63  
64  
65

## Materials and Methods

### 2.1 Materials

N-hydroxysuccinimide (NHS), N-(3-dimethylaminopropyl)-N'-ethylcarbodiimide hydrochloride (EDC), Keyhole limpet hemocyanin (KLH) and  $\alpha$ -lipoic acid were purchased from Sigma-Aldrich (Sigma-Aldrich S.r.l. Milan, Italy). All the other chemicals were commercial samples of the purest quality.

### 2.2. Naphthalene derivative synthesis

Tetraethylene glycol p-toluenesulfonate (100 mg, 0,287 mmol) was added to a round-bottomed flask containing an ice-cold solution of 5 equivalents of N-Methyl-1-naphthalenemethylamine, in 500  $\mu$ L of anhydrous pyridine. The reaction was left to react for 30 minutes under magnetic stirring, then a gentle reflux was applied by heating the mixture with an oil bath. The colour of the reaction mix turned from transparent to pale yellow after the first 30 min, then into amber during the 2 h of reflux. Thin-layer chromatography (TLC) confirmed the formation of the product. The mixture was co-evaporated with anhydrous toluene to eliminate the pyridine, then it was purified by standard acid/base liquid separation to obtain a viscous amber oil, which was further purified by preparative silica TLC (8:2 DCM:MeOH + 0.1% NH<sub>3</sub> solution). The incorporation of the tetra-ethylene glycol linker was confirmed by nuclear magnetic resonance spectroscopy (NMR) experiment. Finally, the product was further transformed to be amino-reactive by incorporation of a reactive NHS moiety. The alcohol previously obtained was left to react overnight at 4°C under vigorous stirring with 1.2 equivalent of NaH, then iodoacetic acid (5 eq.) was added to the reaction mix. The crude product is then dried at rota-vapor and the mix was esterificated in DMF with 10 eq. of TEMED and 5 eq. of NHS. The obtained compound was characterized by <sup>1</sup>H-NMR and the characteristic resonances of the atomic group present in the structure were identified.

### 2.3 Keyhole Limpet Hemocyanin (KLH- NAPHTA) conjugates production

Keyhole limpet hemocyanin (KLH) is a large, multi-subunits, oxygen-carrying metallo-protein extensively used as a carrier protein in the production of antibodies. The KLH was purchased from the Thermo-Fisher and was used in conjugation reaction with the amino reactive naphthalene

1 produced. For the conjugation, the following procedure was used: Naphthalene derivative  
2 containing the reactive group for a fast self-coupling with proteins was dissolved in 10 mM  
3 phosphate buffer at pH 7.4 and incubated with the KLH protein, the molar ratio was 1:100. The  
4 reaction mixture was incubated at room temperature under continuous stirring for 2 hours and then  
5 dialyzed against 0.5 L of 10 mM phosphate buffer at pH 7.4 for 4 days with daily buffer changes.  
6 After the extensive dialysis the conjugate KLH-NAPHTA produced was used as antigen in the  
7 immunization procedure.  
8  
9  
10  
11  
12  
13

#### 14 *2.4 Immunization procedure and purification of IgG anti-Naphthalene*

15 Two rabbits were immunized following a standard protocol of immunization reported in Pennacchio  
16 et al. [26]. For this purpose, intradermal inoculation of KLH- NAPHTA conjugate (1 mg per each  
17 rabbit) was executed. At the end of the immunization process, the rabbits were sacrificed and their  
18 blood collected and centrifuged to separate blood cells from serum. The obtained sera were used for  
19 IgG anti-Naphthalene purification. Soon afterwards, the serum sample was diluted in ratio 1:1 with  
20 binding buffer (Tris-HCl 50 mM pH 7.4) and applied to Protein A resin (Sigma-Aldrich). After an  
21 overnight binding step, the flow-through was eluted and the wash step with 50 mM Tris-HCl pH 7.4  
22 was performed in order to remove the un-binding proteins from the column. After these steps, the  
23 IgG fractions were eluted from column with 0.1 M of Glycine-HCl pH 3.0 and immediately  
24 buffered using a solution of Tris-HCl 1.0 M pH 9.0. In order to estimate the homogeneity and the  
25 molar concentration of the purified total IgG, a gel electrophoresis in denatured condition (SDS-  
26 PAGE) and adsorption spectra were respectively made (data not shown).  
27  
28  
29  
30  
31  
32  
33  
34  
35  
36  
37  
38  
39

#### 40 *2.5 Affinity column preparation of NAPHTA -EAH Sepharose 4B and mono-specific antibody anti-* 41 *Naphtha purification*

42 The affinity column was obtained by conjugating the naphthalene derivative to EAH Sepharose 4B  
43 using the manufacturing instruction. In brief, a 12 mL sample of the resin was washed with H<sub>2</sub>O at  
44 pH 4.5 (160 mL), with 0.5M NaCl (100 mL), and again with H<sub>2</sub>O at pH 4.5 (100 mL). The  
45 Sepharose resin was finally packed into a polystyrene column (50 mL, BIORAD) suspended in 2.0  
46 mL of H<sub>2</sub>O at pH 4.5 and the resulting suspensions were gently shaken. The Naphthalene  
47 derivative, containing in its structure a reactive group for a fast self-coupling with proteins, was  
48 dissolved in 10 mM phosphate buffer at pH 7.4 and incubated with the slurry resin at a molar ratio  
49 of 1:10 for 2 h at room temperature. The slurry resin solution was extensively washed with H<sub>2</sub>O at  
50 pH 4.5, 0.5 M NaCl, then it was treated with 15 mL of 0.1 M AcOH at pH 4.0, 0.5 M NaCl  
51 (blocking buffer) and later with 0.1MTris-HCl at pH 7.0, 0.5 M NaCl (wash buffer). After this step,  
52  
53  
54  
55  
56  
57  
58  
59  
60  
61  
62  
63  
64  
65

1 the resin was washed with the blocking buffer and incubated for 30 min at room temperature.  
2 Finally, the resin was equilibrated with 10 mL of 50 mM Tris-HCl at pH 7.4. The total IgGs  
3 obtained from the Protein A purification step were incubated with the EAH-Naphtha resin  
4 produced. After the incubation step, the column was extensively washed with 50 mM Tris-HCl  
5 pH7.4 in order to remove un-specific binding with the EAH-NAPHTA resin of the IgGs. The  
6 mono-specific IgGs were eluted by strong pH changing (Glycine 50 mM pH 3.0) and the purity and  
7 binding capability of the obtained mono-specific antibodies were evaluated through the SDS-  
8 PAGE. Finally, the concentration of the antibodies at the end of dialyses processes was  
9 spectrophotometrically determined by absorbance measurements at  $\lambda = 278$  nm.  
10  
11  
12  
13  
14  
15  
16

### 17 *2.6 Glutamine-Binding protein- NAPHTA conjugate and ELISA test*

18 The antibodies titer was determined by using indirect ELISA assay, as reported by Pennacchio [26].  
19 In order to avoid interference from the carrier protein in the polyclonal antibody detection process,  
20 NAPHTA derivative (through the same procedure used for KLH- NAPHTA) was conjugated to the  
21 Glutamine binding protein isolated from E. coli [27]. The GlnBP- NAPHTA conjugate (2 mg/ml),  
22 prepared according to Pennacchio [26], diluted 1/200, was dissolved in coating buffer at pH 9.5 (25  
23 mM carbonate/bicarbonate) and was deposited on coat 96-well micro-plates surface in a range of  
24 concentrations from 1.2 ng/mL to 1.7 ng/mL, GlnBP with same concentration was dissolved in  
25 coating buffer and used as negative control. The plate was incubated overnight at 4°C. After this  
26 incubation, it was washed three-times with PBS buffer (0.1 M) containing 0.05% Tween (PBS-T),  
27 pH 7.4 and blocked for 1 hour at room temperature with a solution of 1% milk in PBS-T buffer. The  
28 wells were washed several times with PBS-T after each step, incubated with mono-specific anti-  
29 PFOA antibodies at 37°C for 1 hour and subsequently with horseradish peroxidase-conjugated anti-  
30 rabbit IgG antibodies (diluted 1:12000). This solution was incubated for 1 hour at 37°C. The  
31 enzyme substrate TMB was added, and the colour reaction was quenched after 5 minutes by the  
32 addition of 2.5 M HCl. The absorbance value at 450 nm was measured, plotting the reciprocal of the  
33 antibody dilution against absorbance.  
34  
35  
36  
37  
38  
39  
40  
41  
42  
43  
44  
45  
46  
47  
48  
49

### 50 *2.7 Plasmonic Platform in optical fiber with the experimental setup*

51 The optical platform was realized in a D-shaped plastic optical fiber (POF) sensing region, of 10  
52 mm in length, by a multilayer deposited on the flat exposed POF core (D-shaped sensing region).  
53 The used POF showed a diameter of 1.0 mm, a core of poly-methyl methacrylate (PMMA) with 980  
54  $\mu\text{m}$  in size and a cladding of fluorinated polymer (20  $\mu\text{m}$  of size).  
55  
56  
57  
58

59 The procedure to obtain this plasmonic platform was based only on three steps: first, removing the  
60  
61  
62  
63  
64  
65

1  
2  
3  
4  
5  
6  
7  
8  
9  
10  
11  
12  
13  
14  
15  
16  
17  
18  
19  
20  
21  
22  
23  
24  
25  
26  
27  
28  
29  
30  
31  
32  
33  
34  
35  
36  
37  
38  
39  
40  
41  
42  
43  
44  
45  
46  
47  
48  
49  
50  
51  
52  
53  
54  
55  
56  
57  
58  
59  
60  
61  
62  
63  
64  
65

cladding of POF (along half circumference) by polishing process; second, spin coating (6,000 rpm for 60 seconds) an optical buffer layer on the POF core; finally, sputtering a thin gold film by a Bal-Tec SCD 500 machine. The sputtering process was repeated three times by applying a current of 60 mA for 35 seconds (20 nm of gold for step).

The proposed buffer layer, used to improve the performances and the adherence of the gold film, was a photoresist Microposit S1813, with a refractive index greater than the one of the POF core [16]. To deposit the photoresist buffer layer, we used a spin coater machine in order to obtain a uniform layer. Furthermore, the shape of the resonance curve and the absence of multiple resonance peaks, obtained with the bare gold surface in water, were indirect indications of the uniformity of the photoresist buffer layer. In particular, the multilayer deposited on the D-shaped POF region presented a thickness of the buffer layer of about 1.5  $\mu\text{m}$  and a gold film of 60 nm.

The optical sensor system was completed with a very small size, simple and low-cost equipment, composed by a halogen lamp and a spectrometer connected to a PC. The white light source (halogen lamp, HL-2000-LL, manufactured by Ocean Optics, Dunedin, FL, USA) had an emission range from 360 nm to 1700 nm, whereas the spectrometer (FLAME-S-VIS-NIR-ES, manufactured by Ocean Optics, Dunedin, FL, USA) had a detection range from 350 nm to 1023 nm. We connected the SPR-POF sensor to the equipment, light source and spectrometer by two removable SMA connectors. The SPR curves along with data values were displayed on-line on the computer screen and saved with the help of a software provided by Ocean Optics, setting the integration time at 1,000  $\mu\text{s}$  and the averaging of the scans at 100. The SPR transmission spectra were normalized to the reference spectrum (air as the surrounding medium) by Matlab software [16].

### 2.8 Immobilization process on the chip surface

Following the immobilization procedure reported in Cennamo *et al* [17], the POF surface was sequentially cleaned with: (1) milli-Q water (3 times for 5 minutes) and (2) 10 % of ethanol solution in milli-Q water (3 times for 5 min). Then the surface was pre-treated before the covalently immobilization of mono-specific antibody against NAPHTA. This procedure consists of three different steps: (1) thiol film production, (2) derivatization of the surface by EDC/NHS (3) antibody anti-Naphthalene (anti-NAPHTA) immobilization. Soon afterwards the gold chip was immersed in freshly prepared solution of  $\alpha$ -lipoic acid dissolved in a solution of pure ethanol 10 % in water at the final concentration of 40 mM and incubated at 25°C for 18 h and after this incubation period, the gold-coated surface was washed with milli-Q water (three times). Sequentially, a mixture of EDC/NHS at the final concentrations of 200 mM and 50 mM, were incubated on the chip surface for 20 minutes at RT, then for 2 h at room temperature with an msAb anti-NAPHTA 2 mg/ml (100

1  
2  
3  
4  
5  
6  
7  
8  
9  
10  
11  
12  
13  
14  
15  
16  
17  
18  
19  
20  
21  
22  
23  
24  
25  
26  
27  
28  
29  
30  
31  
32  
33  
34  
35  
36  
37  
38  
39  
40  
41  
42  
43  
44  
45  
46  
47  
48  
49  
50  
51  
52  
53  
54  
55  
56  
57  
58  
59  
60  
61  
62  
63  
64  
65

μl) solution in sodium phosphate buffer 20 mM, pH 7.5. Finally, the chips were washed with potassium phosphate buffer sodium phosphate buffer 20 mM, pH 7.5 and dried with nitrogen gas.

The immobilization process can be observed by the resonance wavelength, when a buffer solution (blank) is present as bulk. In fact, when a bio-layer is added to the gold film, the measured refractive index increases and the resonance wavelength increases, though there is an equal medium as bulk (buffer solution). The shift value due to the antibodies immobilization (post functionalization) was about 15 nm and about 20 nm after the final passivation step. This method has already been reported in our previous work [17].

### 2.9 Naphthalene sample preparation

2 mg/mL of naphthalene crystalline powder was solved into 2 mL of ethanol. 100 μL of this solution was diluted in 10 mL of deionized water. Then the water solution obtained (10 μg/mL naphthalene, 1% ethanol), was sequentially diluted to prepare the samples in a range of concentration from 2.5 to 0.0005 μg/mL. The simulated sea-water matrix samples (in the same range of naphthalene concentration) were obtained by diluting 10 μg/mL naphthalene in 1% ethanol solution with 0,460 M NaCl buffer.

### 2.10 Binding experiments

Experimental results were collected using a simple measuring protocol: about 50 μL of NAPHTA solutions at different concentrations were dropped over the sensing region; after an incubation step (ten minutes at room temperature for bio-interaction between analytes and receptor), a washing step with PBS (buffer) was carried out before the recording of the spectrum (when buffer is present as bulk). This protocol was used to measure the shift of the resonance determined by the specific binding (analyte/receptor interaction) on the sensing area, and not determined by the bulk refractive index changes or by non-specific binding between the gold surface and the analyte. The binding between the receptor on the SPR-POF platform and NAPHTA in real matrices was evaluated in the range from 0.0 to 2500 ppb (2.5 μg/mL).

### 3. Results and Discussion

#### 3.1 Antibody anti- NAPHTA design and production

During the last decade, a general strategy to activate and bind small analytes to an antigenic carrier was developed to produce high specific MREs such as antibody biomolecules [25-32]. This strategy, shown in **Figure 1**, starts from the functionalization of analytes to obtain a more reactive carboxylic/amino derivative for the conjugation with a carrier protein. This strategy gives an immunogenic molecule that produces a significantly higher immunological response. The immunogenic molecule obtained is then used for the production of antibodies.

In this context, a soluble NAPHTA derivative compound was been generated with the aim to obtain antibody molecules able to bind NAPHTA with high affinity. In particular, a retro-synthetic strategy was been planned and three main features were considered: 1) the derivative molecule should have an intact naphthalene scaffold; 2) the derivative molecule should be a not-immunogenic linker for a high water solubility and maintain a correct orientation; 3) the linker should have a reactive moiety for a fast self-coupling with proteins.

Following this strategy in **Figure 2** are reported the  $^1\text{H}$  NMR spectra (**Figure 2A**) and structure of the derivative compound (**Figure 2B**), obtained with the retrosynthetic approach described in the material and method section. The NAPHTA derivative containing a reactive group for a fast self-coupling with proteins was conjugated to the high immunogenic protein keyhole limpet hemocyanin (KLH). The obtained KLH-NAPHTA (**Figure 2C**) conjugate was used to produce a high-affinity antibody, using a standard protocol of immunization. At the end of this process, anti-NAPHTA antibodies (msAb-NAPHTA) were purified from serum through two different chromatography steps (Protein A Sepharose and NAPHTA-EAH Sepharose). Their binding capability to NAPHTA was evaluated. To estimate the titer of the msAb against NAPHTA, an indirect ELISA test was performed. In order to avoid interference from the carrier protein, in the ELISA test, NAPHTA derivative was conjugated to different carrier molecules. For this purpose the GlnBP isolated from *E. coli* was used. Microplate wells were coated with different concentrations of antigens GlnBP-NAPHTA and reacted with serially diluted msAb-NAPHTA. **Figure 3** shows the ELISA results, where the absorbance values at 450 nm are reported, for different concentrations of coated GlnBP-NAPHTA. No signal was registered from non-coated wells, while a positive signal was observed when the msAb dilution of 1 in 12,000 was applied. In order to test the antibody selectivity, the ELISA was also performed using as potential antigens different molecules that are known to be co-pollutants in the seawater, (e.g. PFOA and PFOS) and no cross-reactivity was found.

1  
2  
3  
4  
5  
6  
7  
8  
9  
10  
11  
12  
13  
14  
15  
16  
17  
18  
19  
20  
21  
22  
23  
24  
25  
26  
27  
28  
29  
30  
31  
32  
33  
34  
35  
36  
37  
38  
39  
40  
41  
42  
43  
44  
45  
46  
47  
48  
49  
50  
51  
52  
53  
54  
55  
56  
57  
58  
59  
60  
61  
62  
63  
64  
65

In **Figure 4** the SPR-POF sensor platform with the flow-chart used for the realization is shown. The obtained optical sensor system is small in size, simple and low-cost, being equipped with a halogen lamp and a spectrometer connected to a PC, as already reported in the Section 2.7.

In **Figure 5** the functionalization of the gold surface of the SPR-POF platform is reported. Aiming at obtaining a smart surface to detect the NAPHTA compound, as reported in our previous works [17, 25], the gold surface was sequentially treated with a solution of  $\alpha$ -lipoic acid (a), EDC/NHS (b) and finally with mono-specific antibodies against the NAPHTA (c). At the end of these steps, a passivation procedure of the surface was performed by incubation of GlnBP for 2 h at room temperature (**Figure 5A**). The immobilization of the antibodies on the sensor surface is confirmed by the SPR results: SPR transmission spectra, reported in **Figure 5B**, show a shift (an increase of the resonance wavelength) in presence of the same bulk refractive index, before and after the functionalization procedure. As already reported in Section 2.8, this shift, due to an increase of the refractive index in contact with the gold surface, indicates that the anti- NAPHTA antibodies were immobilized on the gold surface. **Figure 5B** shows a resonance shift value, after the functionalization step, of about 15 nm while the shift amounts to 20 nm after the final passivation step.

### 3.2 NAPHTA detection

In an SPR-POF platform when the refractive index at the gold-dielectric interface increases, the resonance wavelength shifts to the right (increase). When a bio-receptor layer is present on the gold film, the selective recognition and the consequent capture of the target analytes present in a liquid sample, lead to a local increase of the refractive index of the dielectric layer in contact with the metal, therefore the resonance wavelength increases. **Figure 6A** shows the transmission spectra of the SPR-POF with the bio-receptor, normalized to the reference spectrum (with air as the surrounding medium), and obtained at increasing concentrations of NAPHTA in a real sea-water solution. The resonance wavelength is shifted to higher values by increasing the concentration of the analyte (Fig. 6A). **Figure 6B** reports the variation of the resonance wavelength with respect to the blank,  $\Delta\lambda_c$  (nm), versus the analyte amount (ppm), in a semi-log scale, and the fitting by Hill equation reported below [33]:

$$\Delta\lambda_c = \Delta\lambda = \lambda_c - \lambda_0 = \Delta\lambda_{max} \cdot \frac{c^n}{K^n + c^n} \quad (1)$$

where  $\Delta\lambda_{max}$  is the maximum resonance wavelength variation at increasing concentration of

1 naphthalene (the saturation value minus the blank value). The symbol  $c$  indicates the concentration  
2 of the analyte and  $\lambda_c$  indicates the resonance wavelength at  $c$  concentrations. The resonance at  
3 0.0ppb concentration (blank) is indicated as  $\lambda_0$ . The two parameters  $K$  and  $n$  are considered as  
4 descriptors of the standardization curve (Eq. 1), but they can also have a physical meaning [33].  
5 Standardization curves, as the curves described by eq. 1, are commonly used when dealing with  
6 chemical sensors and biosensors. Their physical meaning, in particular the non-linear trend, is  
7 related to the finite number of the specific sites available for adsorption, which leads to a saturation  
8 at high analyte concentrations. In this case, the adsorption takes place according to the Langmuir  
9 adsorption isotherm [33]. The value of  $n$  in the Langmuir sorption model should be equal to 1, and  
10 it is different in case of the presence of cooperative effects.

11 In **Figure 6B**, each experimental point (black square) is the average of 5 subsequent measurements  
12 and the error bars represent the respective standard deviations, whereas the fitting is performed  
13 applying by fitting the Hill equation (OriginPro 8.5, Origin Lab. Corp., Northampton, MA, USA).  
14 The obtained parameters are listed in **Table 1**.

15 The  $\Delta\lambda_0$  value should be not significantly different from 0.0, since it indicates the shift of the  
16 resonance wavelength with the concentration of analyte at 0.0 ppb concentration. The value of  $n$   
17 cannot be considered as significantly different from 1.0 (see Table 1). From Eq. 1 it is possible to  
18 notice that, if  $n \approx 1$  and at low concentration, i.e. at  $c$  much lower than  $K$ , the dose-response curve is  
19 linear, with sensitivity  $\Delta\lambda_{\max}/K$ , defined as the "sensitivity at low concentration", as shown in Eq. 2:

$$\Delta\lambda_c = \frac{\Delta\lambda_{\max}}{K} \cdot c \quad (2)$$

20 Standardization curves, like the curves reported in **Figure 6B**, with the Hill parameters listed in  
21 **Table 1**, are commonly used for biosensors. When the number of receptor sites available for the  
22 combination with the substrate is limited, the physical meaning of the Hill's parameters can be  
23 related to the fact that the adsorption takes place by the combination of the substrate at specific sites  
24 (the adsorption takes place according to the Langmuir adsorption isotherm). The parameter  $K$  of the  
25 Hill equation (Eq. 1 and 2) corresponds to the reciprocal of the affinity constant of the specific sites  
26 of the Langmuir model [33]. The affinity constant ( $K_{\text{aff}}$ ), the sensitivity at low concentration and the  
27 lower detection limits (LOD) of naphthalene in a real sea-water solution are reported in **Table 2**.  
28 The LOD can be calculated by the ratio of three times the standard deviation of the blank.

29 In order to verify the non-specific binding between the sensing layer and the NAPHTA, the  
30 response of SPR-POF sensor without the bio-receptor was tested. **Figure 7** shows the SPR curves

1  
2  
3  
4  
5  
6  
7  
8  
9  
10  
11  
12  
13  
14  
15  
16  
17  
18  
19  
20  
21  
22  
23  
24  
25  
26  
27  
28  
29  
30  
31  
32  
33  
34  
35  
36  
37  
38  
39  
40  
41  
42  
43  
44  
45  
46  
47  
48  
49  
50  
51  
52  
53  
54  
55  
56  
57  
58  
59  
60  
61  
62  
63  
64  
65

obtained with different concentrations of NAPHTHA in real solution. In this case, we used a range of NAPHTHA concentration wider than the saturation value (around 10 ppb). The results obtained show that, as a consequence of the concentration increase, the shift of the resonance wavelength was not registered.

#### **4. Conclusion**

Aiming at detecting naphthalene in seawater, we designed a novel SPR-POF sensor that combines a novel antibody layer with a plasmonic platform in plastic optical fibers. The procedure used for the bio-receptor design and production allows to obtain very high affinity antibodies against the NAPHTHA and this characteristic was used to develop the SPR-POF biosensor. The binding tests were realized on laboratory and simulated real matrix samples. The selective recognition of NAPHTHA, in a liquid sample by antibody layer, displayed an increase of the resonance wavelength. The obtained results showed that the assay is selective and able to sense the presence of a very low amount of NAPHTHA, exhibiting a LOD of 0.76 ng/mL (0.76 ppb), a value that is lower than the one fixed by the European Union regulations. In the future, after these preliminary laboratory results, the remote sensing capabilities offered by optical fibers could be exploited for on-site and real-time monitoring of the naphthalene concentration in sea-water.

#### **Acknowledgments**

This work was funded by the EUFP7 program under grant agreement N° 614088- Mariabox project.

## Reference

- [1] USEPA, compendium of methods for determination of toxic organic compounds in ambient air, Center for Environmental Research Information; Office of Research and Development, U.S. Environmental Protection Agency; Cincinnati, OH 45268 Second Edition (January, 1999).
- [2] WHO, IARC Monographs on the evaluation of carcinogenic risks to humans - some traditional herbal medicines, some mycotoxins, naphthalene and styrene, ed.82, IARC Press, Lyon, France (2002).
- [3] WHO, Development of WHO Guidelines for indoor air quality, WHO Regional Office for Europe, Copenhagen, Denmark (2006).
- [4] C.R. Jia, S. Batterman, A critical review of naphthalene sources and exposures relevant to indoor and outdoor air, *Int. J. Environ. Res. Public Health* 7 (2010) 2903-2939.
- [5] J.J. Schauer, M.J. Kleeman, G.R. Cass, B.R. Simoneit, Measurement of emissions from air pollution sources. 5. C1-C32 organic compounds from gasoline-powered motor vehicles, *Environ Sci Technol* 36(6) (2002) 1169-80.
- [6] S.D. Shah, T.A. Ogunyoku, J.W. Miller, D.R. Cocker, 3rd, On-road emission rates of PAH and n-alkane compounds from heavy-duty diesel vehicles, *Environ Sci Technol* 39(14) (2005) 5276-84.
- [7] Helvécio C. Menezes, Breno P. Paulo, Nathália T. Costa, Z.L. Cardeal, New method to determination of naphthalene in ambient air using cold fiber-solid phase microextraction and gas chromatography-mass spectrometry *Microchemical Journal* 109 (2013) 93-97.
- [8] K. Hasegawa, H. Nozawa, I. Yamagishi, K. Watanabe, S. O., Simple analysis of naphthalene in human whole blood and urine by headspace capillary gas chromatography with large-volume injection, *Forensic Toxicology* 27(2) (2009) 98-102.
- [9] R. Lindahl, A.S. Claesson, M.A. Khan, J.O. Levin, Development of a method for the determination of naphthalene and phenanthrene in workplace air using diffusive sampling and thermal desorption GC-MS analysis, *Ann Occup Hyg* 55(6) (2011) 681-7.
- [10] M.A. Hossain, F. Yeasmin, S.M.M. Rahman, M.S. Rana, Gas chromatograph-mass spectrometry determination of carcinogenic naphthalene, anthracene, phenanthrene and fluorene in the Bangsai river water of Bangladesh, *Arabian Journal of Chemistry* 9(1) (2016) S109-S113.
- [11] J.M. Shamar, Separation and identification of naphthalene, acenaphthylene, pyrene, benz{a}anthracene and 1,3,2,4-dibenzanthracene, *Journal of Al-Nahrain University* 12 (4) (December, 2009) 14-24
- [12] Cheng-Yu Wang, Frank and Edwards, K. E., Separation of C2-naphthalenes by gas chromatography Fourier transform infrared spectroscopy (GC FT-IR): Two-Dimensional Separation Approach, *Anal. Chem.* 79 (2007) 106-112.
- [13] John M. Hayes, G.J. Small, rotationally cooled laser-induced fluorescence/gas chromatography, *Anal. Chem.* 54( 7) (1982) 1202-1204.
- [14] Nicola Zanca, Andrew T. Lambe, Paola Massoli, Marco Paglione, David R. Croasdale, Yatish Parmar, Emilio Tagliavini, Stefania Gilardoni, a.S. Decesari, Characterizing source fingerprints and ageing processes in laboratory-generated secondary organic aerosols using proton-nuclear magnetic resonance (1H-NMR) analysis and HPLC HULIS determination, *Atmos. Chem. Phys.* 17 (2017) 10405-10421.
- [15] Ulrich Boesl, Laser mass spectrometry for environmental and industrial chemical trace analysis, *Journal of mass spectrometry* 35(3) (2000) 289-304.
- [16] N. Cennamo, D. Massarotti, L. Conte, L. Zeni, Low cost sensors based on SPR in a plastic optical fiber for biosensor implementation, *Sensors (Basel)* 11(12) (2011) 11752-60.
- [17] N. Cennamo, L. Zeni, P. Tortora, M.E. Regonesi, A. Giusti, M. Staiano, S. D'Auria, A. Varriale, A high sensitivity biosensor to detect the presence of perfluorinated compounds in environment, *Talanta* 178 (2018) 955-961.

- 1 [18] L. Bilro, N. Alberto, J.L. Pinto, R. Nogueira, Optical sensors based on plastic fibers, *Sensors* 12 (2012) 12184-12207.
- 2 [19] Y. Jin, A. M. Granville, Polymer Fiber Optic Sensors - A Mini Review of their synthesis and  
3 applications, *J. Biosens. Bioelectron.* 7: 194 (2016) 1-11.
- 4 [20] V.V.R. Sai, T. Kundu, S. Mukherji, Novel U-bent fiber optic probe for localized surface  
5 plasmon resonance based biosensor, *Biosens Bioelectron* 24 (2009) 2804.
- 6 [21] N. Cennamo, A. Varriale, A. Pennacchio, M. Staiano, D. Massarotti, L. Zeni, S. D'Auria, An  
7 innovative plastic optical fiber based biosensor for new bio/applications. The case of celiac disease,  
8 *Sens. Act. B: Chem.* 176 (2013) 1008–1014.
- 9 [22] N. Cennamo, G. Alberti, M. Pesavento, G. D'Agostino, F. Quattrini, R. Biesuz, L. Zeni, A  
10 simple small size and low cost sensor based on surface plasmon resonance for selective detection of  
11 Fe(III), *Sensors* 14 (2014) 4657-4671.
- 12 [23] N. Cennamo, M. Pesavento, L. Lunelli, L. Vanzetti, C. Pederzoli, L. Zeni, L. Pasquardini, An  
13 easy way to realize SPR aptasensor: A multimode plastic optical fiber platform for cancer  
14 biomarkers detection, *Talanta* 140 (2015) 88–95.
- 15 [24] A. Aray, F. Chiavaioli, M. Arjmand, C. Trono, S. Tombelli, A. Giannetti, N. Cennamo, M.  
16 Soltanolkotabi, L. Zeni, F. Baldini, SPR-based plastic optical fibre biosensor for the detection of C-  
17 reactive protein in serum, *J Biophotonics* 9 (2016)1077–1084.
- 18 [25] N. Cennamo, S. Di Giovanni, A. Varriale, M. Staiano, F. Di Pietrantonio, A. Notargiacomo, L.  
19 Zeni, S. D'Auria, Easy to use plastic optical fiber-based biosensor for detection of butanal, *PLoS*  
20 *ONE* 10(3) (2015) e0116770.
- 21 [26] A. Pennacchio, A. Varriale, M.G. Esposito, A. Scala, V.M. Marzullo, M. Staiano, S. D'Auria,  
22 A rapid and sensitive assay for the detection of benzylpenicillin (PenG) in milk, *PLoS ONE* 10(7)  
23 (2015) e0132396.
- 24 [27] M. Staiano, V. Scognamiglio, M. Rossi, S. D'Auria, O.V. Stepanenko, I.M. Kuznetsova, K.K.  
25 Turoverov, Unfolding and refolding of the glutamine-binding protein from *Escherichia coli* and its  
26 complex with glutamine induced by guanidine hydrochloride, *Biochemistry* 44(15) (2005) 5625-33.
- 27 [28] M. De Champdoré, P. Bazzicalupo, L. De Napoli, D. Montesarchio, G. Di Fabio, I. Coccozza,  
28 A. Parracino, M. Rossi, S. D'Auria, A new competitive fluorescence assay for the detection of  
29 patulin toxin, *Anal Chem* 15(79(2) ) (2007) 751-757.
- 30 [29] A. Varriale, V.M. Marzullo, S. Di Giovanni, A. Scala, A. Capo, A. Majoli, A. Pennacchio, M.  
31 Staiano, S. D'Auria, On the possibility of ephedrine detection: time-resolved fluorescence resonance  
32 energy transfer (FRET)-based approach, *Anal Bioanal Chem* 408(23) (2016) 6329-36.
- 33 [30] S. Di Giovanni, A. Varriale, V.M. Marzullo, G. Ruggiero, M. Staiano, A. Secchi, L. Pierno,  
34 A.M. Fiorello, S. D'Auria, Determination of benzyl methyl ketone - a commonly used precursor in  
35 amphetamine manufacture, *Anal. Methods* 4 (2012) 3558-3564.
- 36 [31] A. Varriale, K. Bonnot, S. Peransi, A. Scala, S. D'Auria, Self-oriented monolayer  
37 immobilization of ovalbumin and *B. cereus* antibody molecules on a chemically modified surface of  
38 silicon nitride fosters the enhancement of capture of bio-agents, *Colloids Surf B Biointerfaces* 148  
39 (2016) 585-591.
- 40 [32] A. Pennacchio, A. Varriale, M.G. Esposito, M. Staiano, S. D'Auria, A near-infrared  
41 fluorescence assay method to detect patulin in food, *Anal Biochem* 481 (2015) 55-9.
- 42 [33] B.I. Burganov, A.V. Lobanov, I.A. Borisov, A.N. Reshetilov, Criterion for Hill equation  
43 validity for description of biosensor calibration curves, *Anal. Chim. Acta* 427 (2001) 11-19.
- 44  
45  
46  
47  
48  
49  
50  
51  
52  
53  
54  
55  
56  
57  
58  
59  
60  
61  
62  
63  
64  
65

1  
2  
3 **Figure legend**  
4

5 **Figure 1.** Flowchart of the strategy used for antibodies production, purification and quantification.  
6

7 **Figure 2.** (A) <sup>1</sup>H NMR spectrum of the naphthalene derivative. (B) Water soluble and self-  
8 conjugate naphthalene derivative. (C) 2. Scheme of conjugation reaction between the KLH and  
9 naphthalene derivative, the reaction was performed at RT, at pH 6.0 for 2 h.  
10  
11

12 **Figure 3.** Indirect ELISA test results obtained using msAb anti-NAPTHA. The assay was  
13 performed in the Tris-borate buffer in the presence of 0.005% Tween and 1% milk. Temperature  
14 was 25 °C.  
15

16 The dilution of anti-NAPTHA was 1:12,000.  
17

18 **Figure 4.** Plasmonic platform in POF with the experimental setup and the description of the needed  
19 steps to realize it.  
20  
21

22 **Figure 5.** Gold surface functionalization processes. Resonance spectra were acquired in buffer  
23 solution (PBS) obtained before and after the functionalization and passivation processes.  
24  
25

26 **Figure 6.** SPR spectra acquired to naphthalene detection. (A) SPR spectra obtained by SPR-POF  
27 *with* the bio-receptor at different concentrations of naphthalene in real seas water matrices (460 mM  
28 NaCl), in the range from 0.0 to 2500 ppb. (B) Plasmon resonance wavelength shift ( $\Delta\lambda_c$ ) versus  
29 concentration of naphthalene (ppb) in semi-logarithmic axes, and Hill equation fitting of the  
30 experimental data.  
31  
32

33  
34 **Figure 7.** SPR spectra obtained by SPR-POF *without the* bio-receptor at different concentrations of  
35 naphthalene in real sea-water matrices.  
36  
37  
38  
39  
40  
41  
42  
43  
44  
45  
46  
47  
48  
49  
50  
51  
52  
53  
54  
55  
56  
57  
58  
59  
60  
61  
62  
63  
64  
65

**Table 1.** Hill parameters of naphthalene detection in real solution by SPR-POF biosensor

$\Delta\lambda_0$ [nm]		$\Delta\lambda_{\max}$ [nm]		K [ppb]		n		Statistics	
Value	Standard Error	Value	Standard Error	Value	Standard Error	Value	Standard Error	Reduced Chi-Sqr	Adj. R-Square
-1.3	14.8	7.36	0.898	0.149	0.533	0.968	1.27	65.719	0.912

**Table 2.** Chemical parameters for naphthalene detection in real solution by SPR-POF biosensor

	<i>Parameters</i>	<i>Value</i>
SPR-POF biosensor	$K_{\text{aff}}$ [ ppb <sup>-1</sup> ] ( $K_{\text{aff}}=1/K$ )	6.71
	Sensitivity at low $c$ [nm/ppb] (Sensitivity at low $c = \Delta\lambda_{\text{max}} / K$ )	58.12
	LOD [ ppb ] (3*standard deviation of blank / Sensitivity at low $c$ )	0.76

Figure 1  
[Click here to download high resolution image](#)

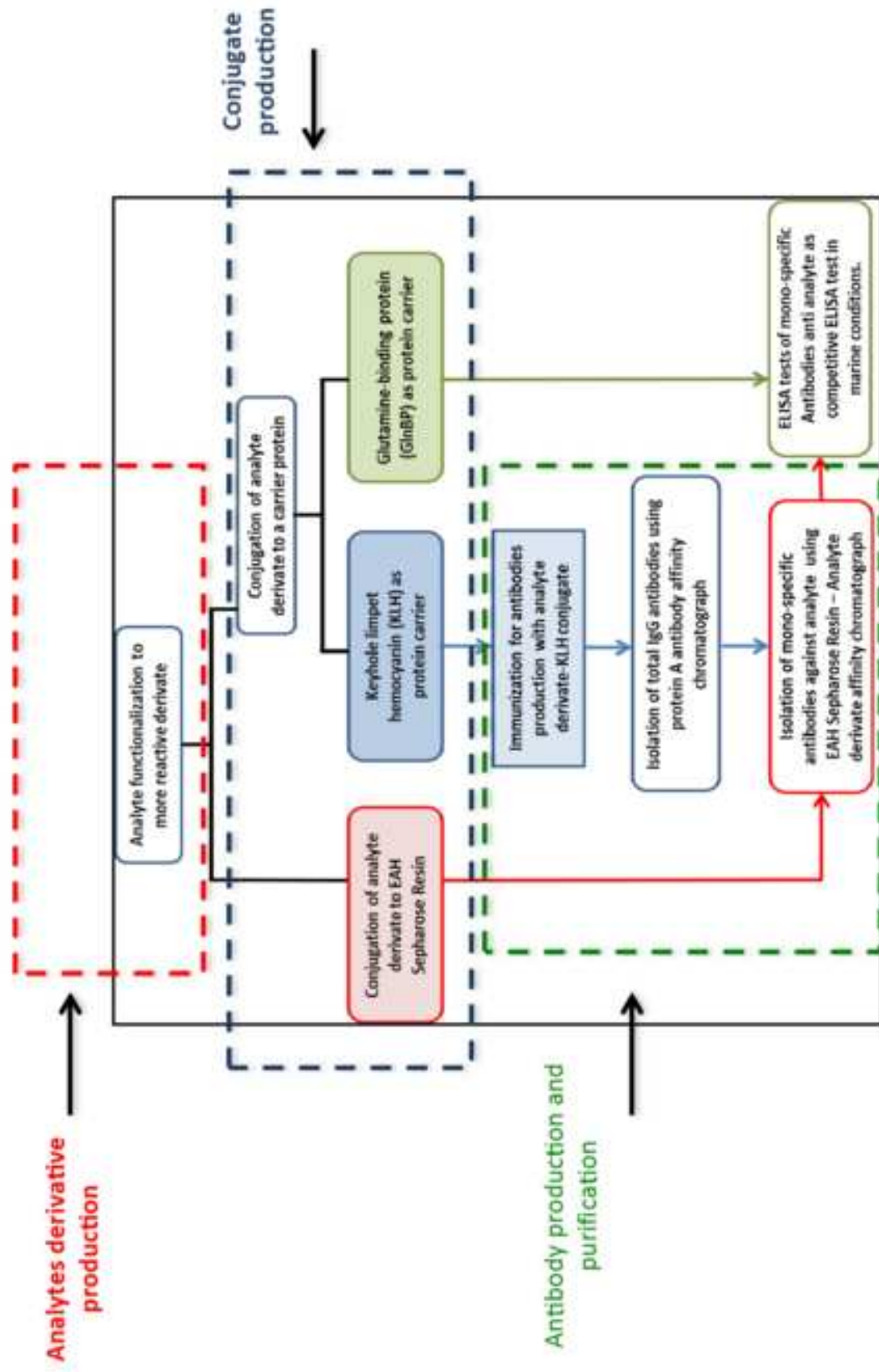


Figure 2  
[Click here to download high resolution image](#)

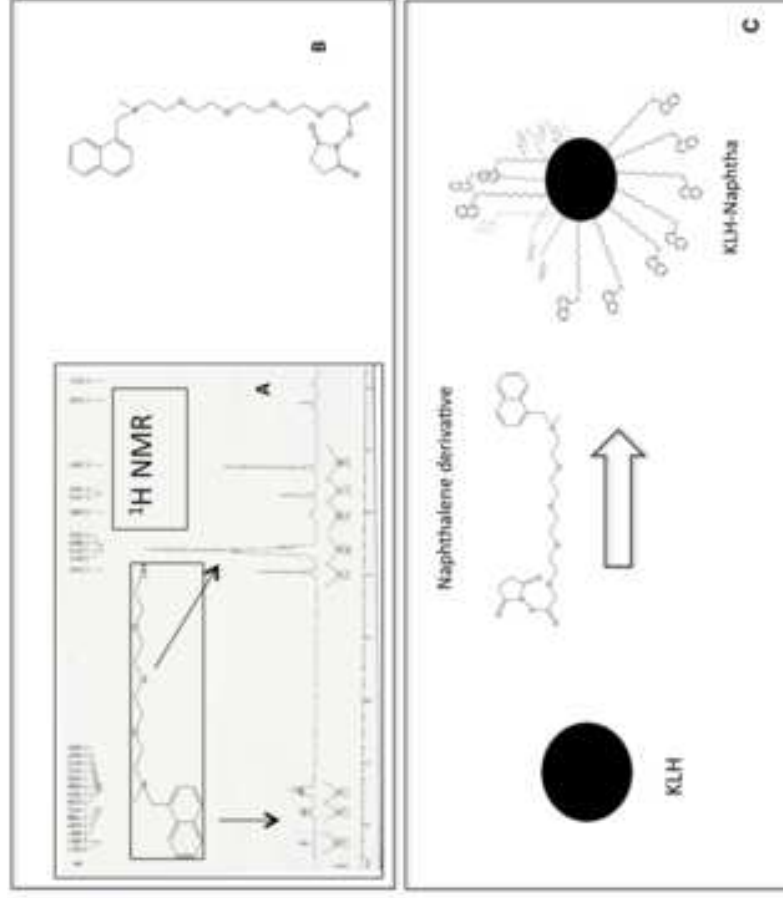


Figure 3  
[Click here to download high resolution image](#)

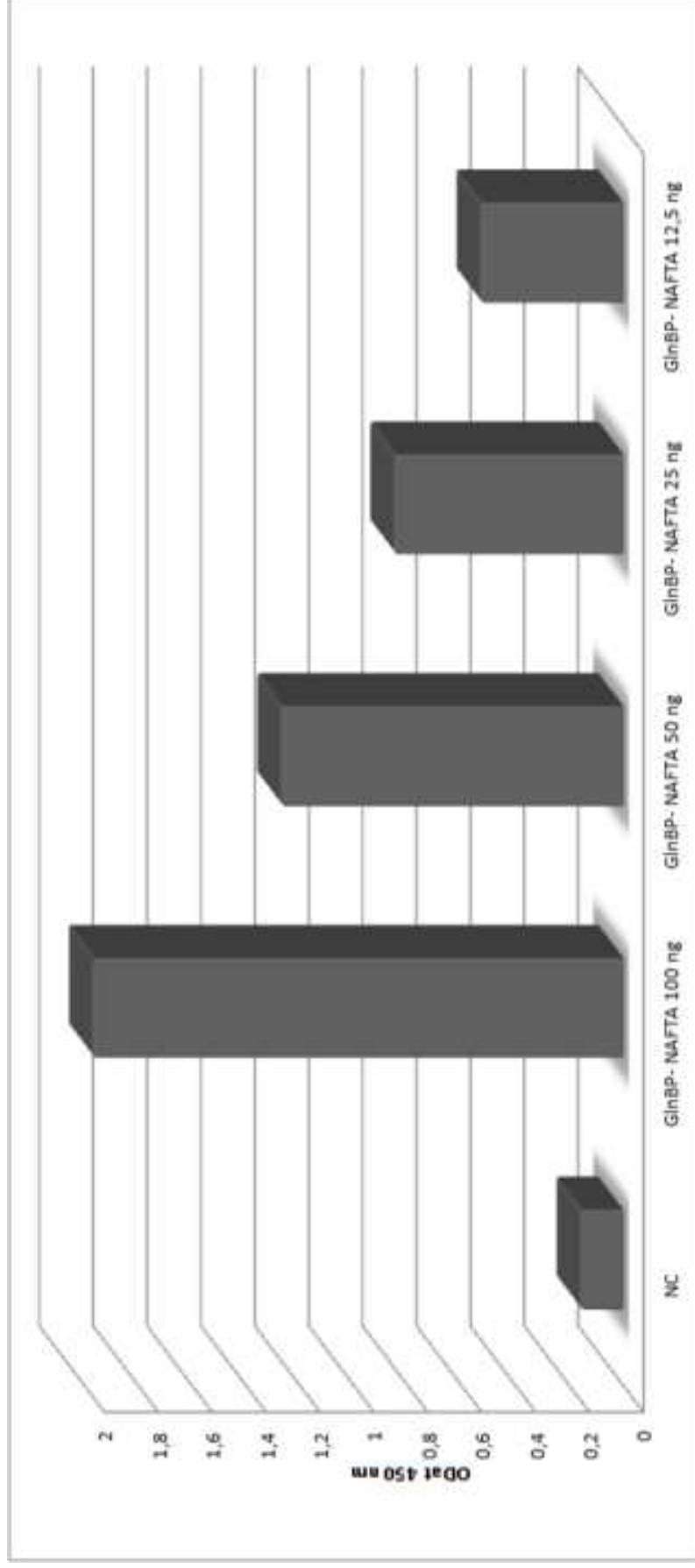


Figure 4  
[Click here to download high resolution image](#)

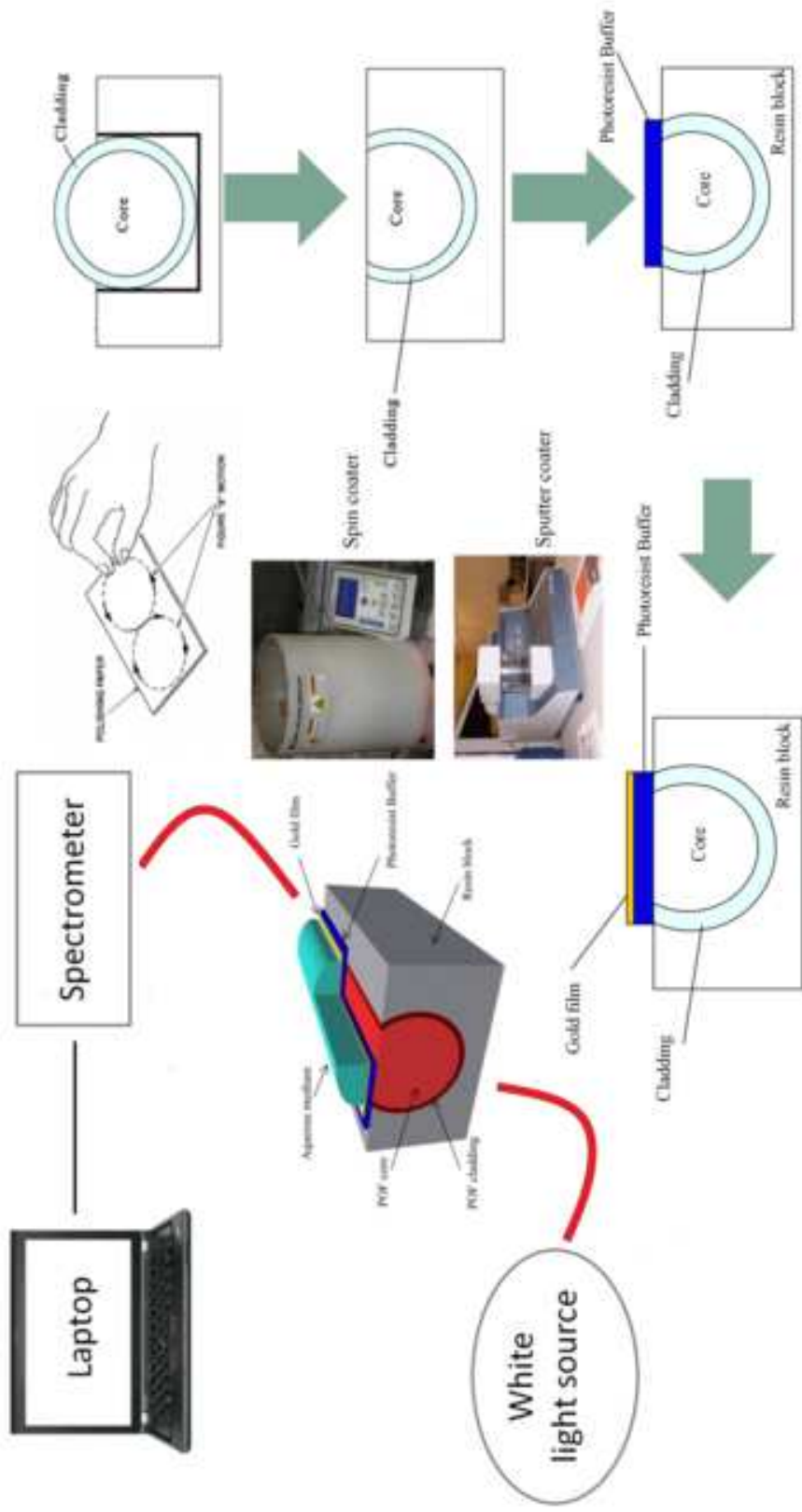


Figure 5  
[Click here to download high resolution image](#)

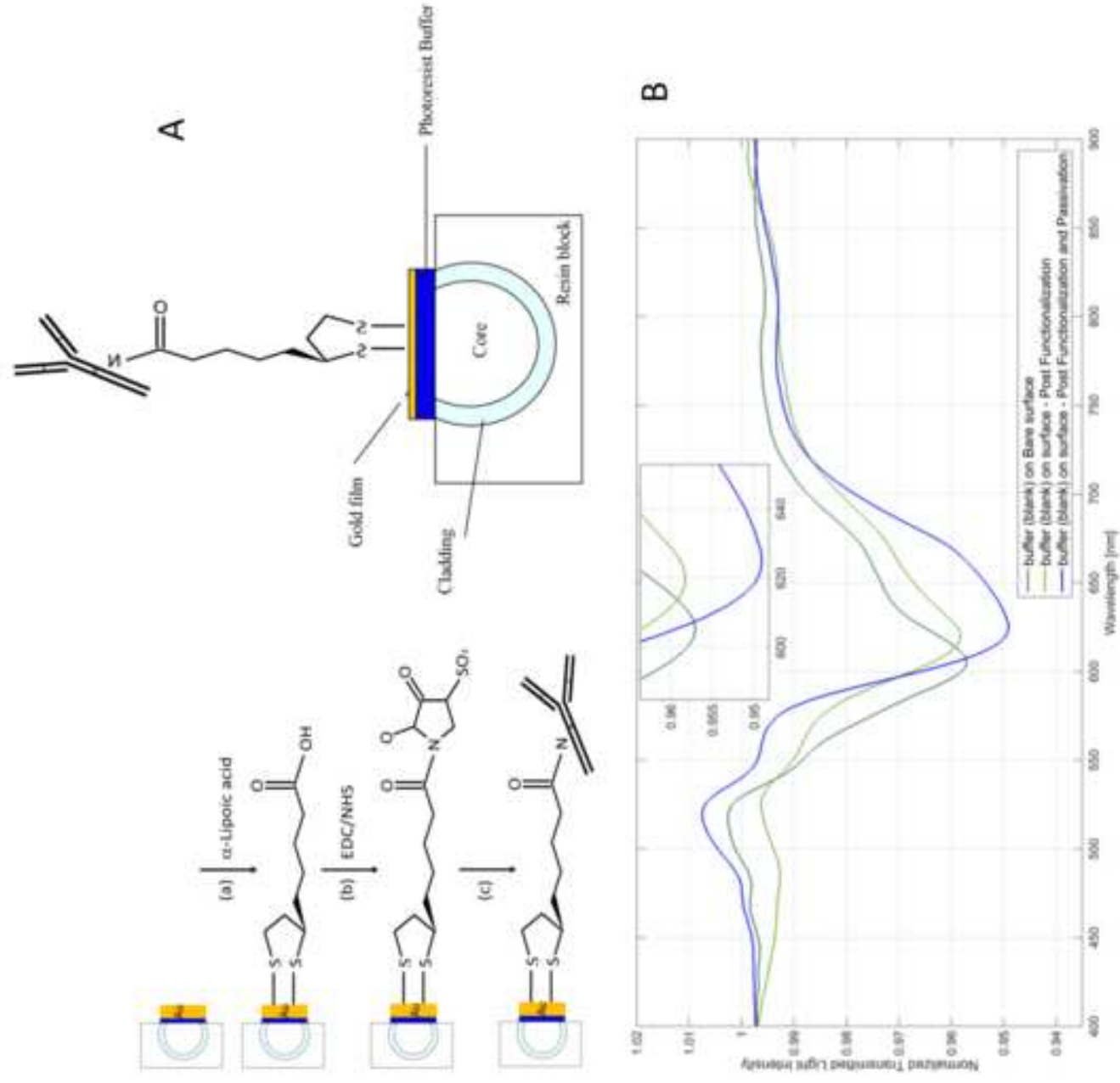
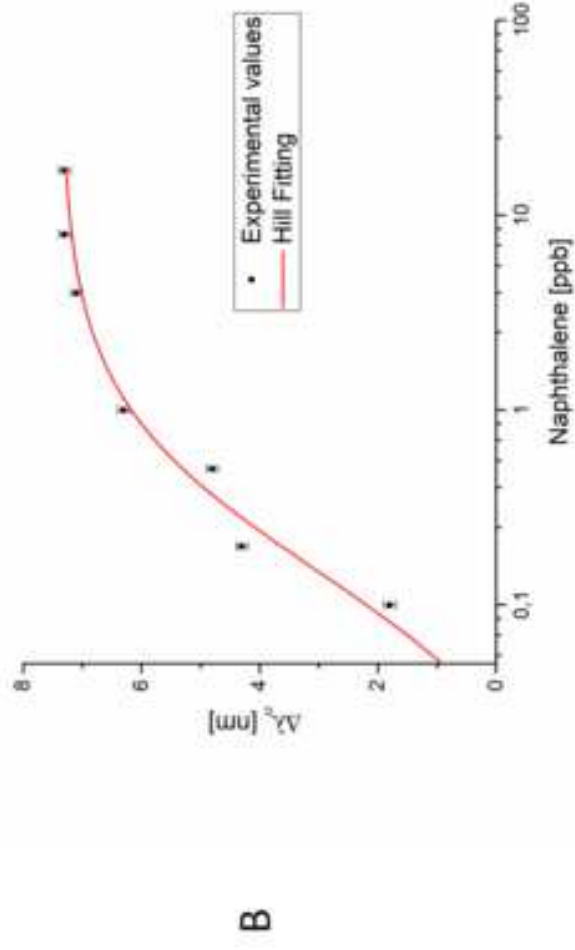
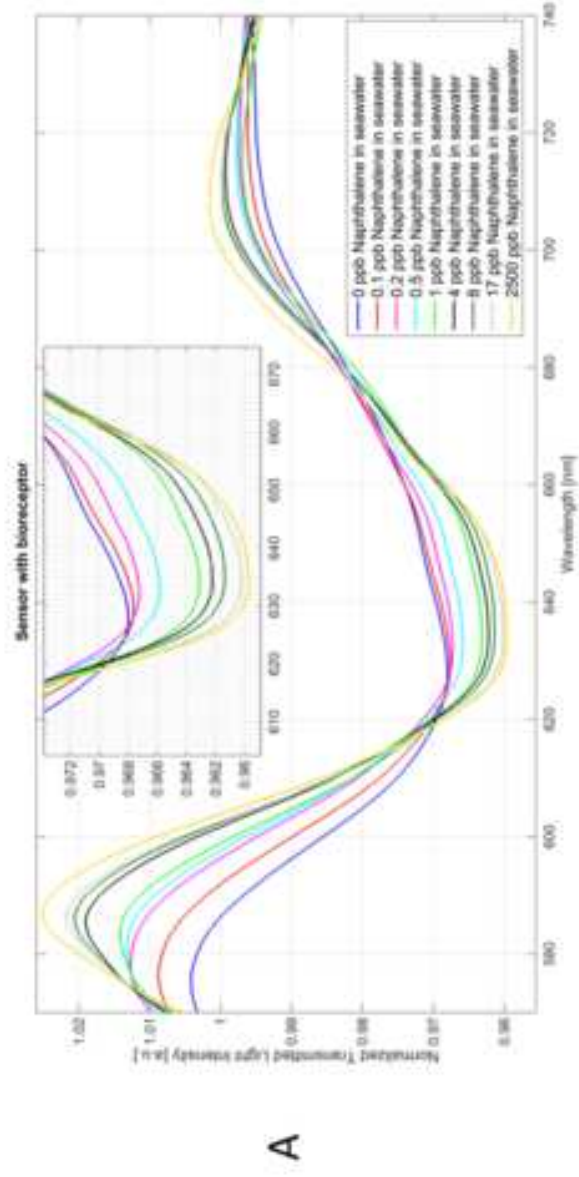
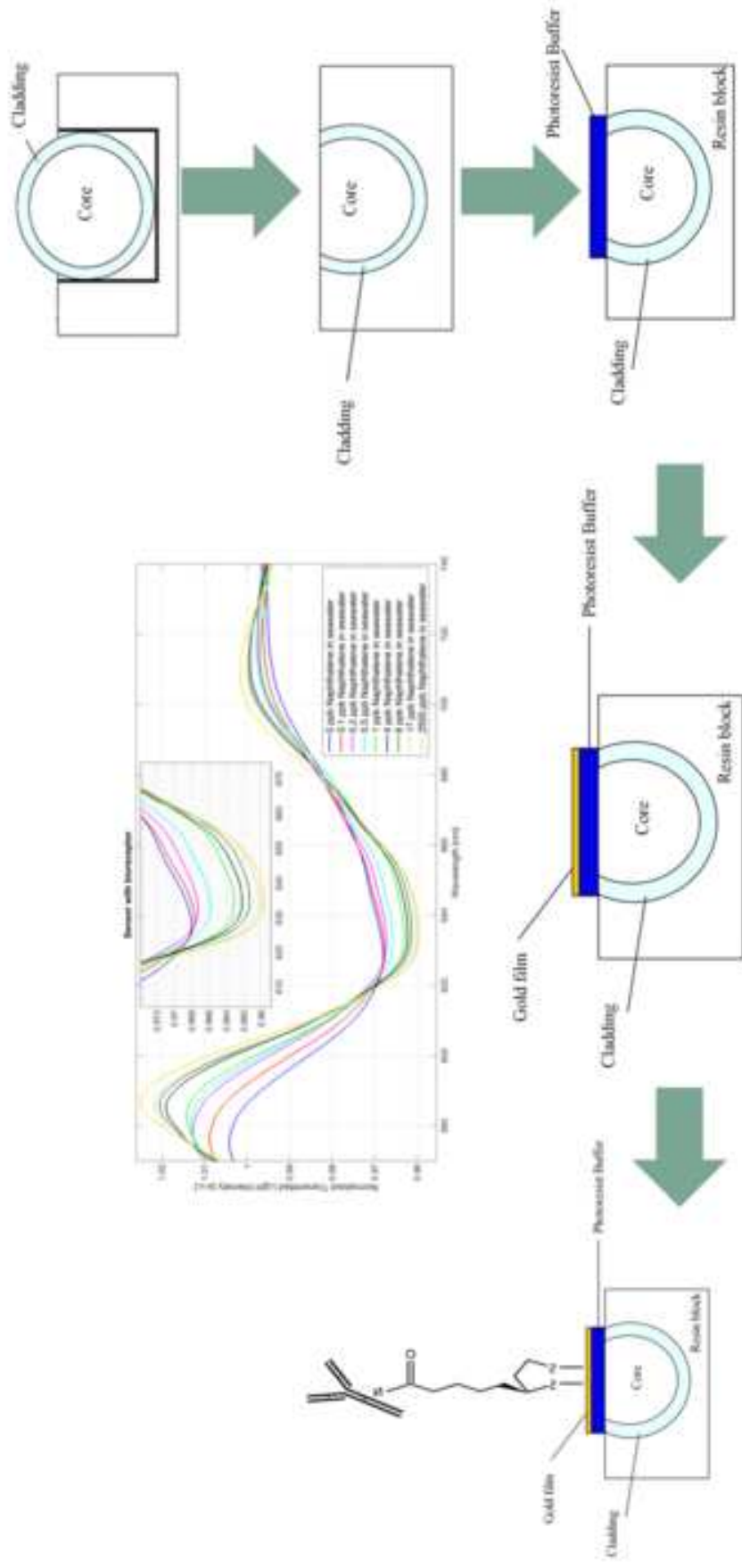


Figure 6  
[Click here to download high resolution image](#)







## \*Checklist

- 1 Cover Letter
- 2 Novelty Statement
- 3 Highlights
- 4 Manuscript
- 5 Tables n° 2
- 6 Figures n° 7
- 7 Graphical Abstract
- 8 List of Three Potential Reviewers